

## Winos from natural SUSY at the high luminosity LHC

Howard Baer<sup>1,\*</sup>, Vernon Barger<sup>2,†</sup>, Xerxes Tata<sup>3,‡</sup> and Kairui Zhang<sup>2,§</sup>

<sup>1</sup>*Homer L. Dodge Department of Physics and Astronomy, University of Oklahoma, Norman, Oklahoma 73019, USA*

<sup>2</sup>*Department of Physics, University of Wisconsin, Madison, Wisconsin 53706 USA*

<sup>3</sup>*Department of Physics and Astronomy, University of Hawaii, Honolulu, Hawaii 53706 USA*



(Received 23 October 2023; accepted 4 January 2024; published 25 January 2024)

In natural supersymmetric models defined by no worse than a part in thirty electroweak fine-tuning, winos and binos are generically expected to be much heavier than Higgsinos. Moreover, the splitting between the Higgsinos is expected to be small, so that the visible decay products of the heavier Higgsinos are soft, rendering the Higgsinos quasi-invisible at the LHC. Within the natural supersymmetry (SUSY) framework, heavy electroweak gauginos decay to  $W$ ,  $Z$  or  $h$  bosons plus Higgsinos in the ratio  $\sim 2:1:1$ , respectively. This is in sharp contrast to models with a binolike lightest superpartner and very heavy Higgsinos, where the charged (neutral) wino essentially always decays to a  $W$  ( $h$ ) boson and an invisible bino. Wino pair production at the LHC, in natural SUSY, thus leads to  $VV$ ,  $Vh$  and  $hh + \cancel{E}_T$  final states ( $V = W, Z$ ) where, for TeV scale winos, the vector bosons and  $h$  daughters are considerably boosted. We identify eight different channels arising from the leptonic and hadronic decays of the vector bosons and the decay  $h \rightarrow b\bar{b}$ , each of which offers an avenue for wino discovery at the high luminosity LHC (HL-LHC). By combining the signal in all eight channels we find, assuming  $\sqrt{s} = 14$  TeV and an integrated luminosity of  $3000 \text{ fb}^{-1}$ , that the discovery reach for winos extends to  $m(\text{wino}) \sim 1.1$  TeV, while the 95% CL exclusion range extends to a wino mass of almost 1.4 TeV. We also identify ‘‘Higgsino specific channels’’ which could serve to provide  $3\sigma$  evidence that winos lighter than 1.2 TeV decay to light Higgsinos rather than to a binolike lightest supersymmetric particle, should a wino signal appear at the HL-LHC.

DOI: [10.1103/PhysRevD.109.015027](https://doi.org/10.1103/PhysRevD.109.015027)

### I. INTRODUCTION

The search for supersymmetric partners of Standard Model (SM) particles at high energy colliders has been on the cutting edge of high energy physics ever since it was realized that supersymmetry could stabilize the weak scale provided that the superpartner masses were not very far above the TeV scale [1–4]. Indeed the discovery [5,6] of the seemingly SM-like Higgs boson makes it even more urgent to discover why radiative corrections do not drive its mass to the scale of the most massive particles that couple to the particles of the SM. Even ignoring gravity on the grounds that we may not know how to incorporate it into a quantum framework, there are a number of reasons to suppose that

there are new particles (that couple to the Higgs sector) with masses between the weak scale and the Planck scale. Though it remains a speculation at the present time, arguably the most compelling theoretical reason for new particles is the Grand Unification of the electroweak and strong interactions into a single gauge interaction at the scale  $M_{\text{GUT}}$ . Nonzero neutrino masses may also have their origin in heavy (SM singlet) particles if these acquire their masses via the so-called see-saw mechanism as opposed to tiny dimensionless Yukawa couplings: implications of this for the hierarchy problem are discussed in Ref. [7]. There could also be new particles at a scale associated with the origin of flavor. Regardless of what the new physics is, radiative corrections would generically make the Higgs boson squared mass *quadratically sensitive* to this new scale, except in a supersymmetric theory with the supersymmetry (SUSY) breaking scale well below the scale associated with the new physics: in this case, the Higgs boson mass squared would only be logarithmically sensitive to the UV scale, but quadratically sensitive to the scale of SUSY breaking.

These considerations had led to much hope that superpartners would show up in direct searches at the LHC. As is well known, this has not happened, and the nonobservation of an excess of events in various channels has led only to

\*baer@ou.edu

†barger@pheno.wisc.edu

‡tata@phys.hawaii.edu

§kzhang89@wisc.edu

*Published by the American Physical Society under the terms of the Creative Commons Attribution 4.0 International license. Further distribution of this work must maintain attribution to the author(s) and the published article's title, journal citation, and DOI. Funded by SCOAP<sup>3</sup>.*

lower limits of  $\sim 2.3$  TeV on the masses of strongly interacting gluinos decaying to third generation quarks, of 1.4–1.8 TeV on squarks (assuming an approximate degeneracy among squark flavors), and about 1.3 TeV on the top squark [8–11]. There are also lower bounds of several hundred GeV to just over a TeV on the masses of electroweakly interacting sleptons and the winos [12–19]. It should be noted though that these limits are mostly obtained in simplified models, assuming  $R$ -parity conservation, specific decay modes of the parent sparticle, and a large mass gap between the particle being searched for and the lightest supersymmetric particle (LSP) often assumed to be the lightest neutralino.<sup>1</sup>

The absence of signals at the LHC has led some authors to suggest that the supersymmetry is unable to explain the value of the Higgs boson mass without resorting to some degree of fine-tuning, typically stated to be at a parts per mille level. These authors evaluate the sensitivity of  $m_Z^2$ , which serves the electroweak scale and is calculable in terms of model parameters, to the *independent* parameters,  $a_i$ , of the model:  $\Delta = \max_i | \frac{a_i}{M_Z^2} \frac{\partial M_Z^2}{\partial a_i} |$  [20–23]. Typically, most of the parameters in any model  $a_i$  have to do with soft supersymmetry breaking (SSB), with the superpotential Higgsino mass,  $\mu$ , often the sole dimensionful supersymmetric parameter. In the absence of an understanding of how superpartners acquire their masses, it is not possible to know how the SSB parameters are correlated in the underlying theory. It has, however, been pointed out that ignoring correlations among the parameters can lead one to overestimate the degree of fine-tuning (by up to a factor  $10^3$  [24]), and prematurely cause us to discard perfectly viable models [25,26]. For this reason, we follow a different path to assess the fine-tuning in the minimal supersymmetric Standard Model (MSSM).

Again, we take the experimental value of the  $Z$ -boson mass to represent the magnitude of weak scale, but this time express it in terms of Lagrangian parameters determined at the weak scale via the minimization of the potential in the Higgs sector as

$$m_Z^2/2 = \frac{m_{H_d}^2 + \Sigma_d^d - (m_{H_u}^2 + \Sigma_u^u) \tan^2 \beta}{\tan^2 \beta - 1} - \mu^2. \quad (1)$$

Here,  $m_{H_u}^2$  and  $m_{H_d}^2$  are the Higgs soft breaking mass terms,  $\mu$  is the (SUSY preserving) superpotential Higgsino mass parameter, and the  $\Sigma_d^d$  and  $\Sigma_u^u$  terms include an assortment of loop corrections that are typically most sensitive to third generation sfermion and gaugino masses (see Appendixes of Refs. [27,28] and also see [29] for leading two-loop corrections). We then require that none of the individual terms on the right-hand side is much

larger than  $m_Z^2/2$ , i.e., there are no large cancellations necessary between the supersymmetric term  $\mu^2$  and the SSB terms (or for that matter between the SSB terms in various sectors) that presumably have very different physics origins [30]. With this in mind, we use the electroweak fine-tuning measure [27,31]

$$\Delta_{\text{EW}} = |C_{\text{max}}|/(m_Z^2/2), \quad (2)$$

where  $|C_{\text{max}}|$  is the largest (absolute) term on the right-hand-side of Eq. 1. It has been argued that (modulo some technical caveats),  $\Delta_{\text{EW}} \leq \Delta$ , with the inequality being saturated only for specific correlations between the parameters [26], and further, that  $\Delta_{\text{EW}}$  measures the minimum fine-tuning for a given sparticle spectrum. This makes  $\Delta_{\text{EW}}$  a very conservative estimate of fine-tuning and precludes the possibility of discarding a model even in the presence of correlations among the parameters. We adopt  $\Delta_{\text{EW}} \lesssim 30$  as our criterion for naturalness.

We note here that it has been suggested that notions of stringy naturalness [32] applied to the landscape of string theory vacua, together with the anthropic requirement that a diversity of nuclei form—this anthropic requirement requires that the value of  $m_Z$  be no larger than a factor  $\sim 4$  of its observed value [33]—lead to SUSY models with values of  $\Delta_{\text{EW}} \lesssim 30$  and heavy superpartners (other than light Higgsinos): see Ref. [34] for a review, and for references to the original literature. The reader who does not subscribe to these landscape considerations may view  $\Delta_{\text{EW}} \lesssim 30$  as in between 10 (accidental cancellations of an order of magnitude are known, e.g., the decay rate of orthopositronium includes a factor of  $\pi^2 - 9$ ) and 100 (presumably too large to be attributed to an accidental cancellation). The reader who does not wish to entertain any notions of naturalness may disregard the discussion of the last two paragraphs, and view our analysis as a search for winos in models with light Higgsinos, i.e., where  $|\mu| \ll M_{1,2}$ , where  $M_{1,2}$  are the bino and wino mass parameters at the weak scale.

Requiring  $\Delta_{\text{EW}} < 30$  (this ensures small  $\mu$ ) immediately implies that each of the contributions in Eq. (1) is no bigger than a factor of a few relative to  $m_Z$ . Specifically,

- (1) The  $\mu$  parameter has a magnitude smaller than  $\sim 350$  GeV, so that the Higgsinos are expected to be in the 110–350 GeV range, with the lightest neutral Higgsino being the LSP.
- (2) The finite radiative corrections  $\Sigma_u^u$  have the same upper bound, which requires the top squarks to be bounded above by  $\sim 3$  TeV and the gluino by  $\sim 6$ – $9$  TeV [35], so these can all be well beyond the discovery reach of even the high luminosity LHC (HL-LHC), about 2.8 TeV for the gluino [36] and 1.3–1.7 TeV [37,38] for the stop, depending on how the stop is assumed to decay.

<sup>1</sup>There are also stringent limits on sparticle masses in  $R$ -parity violating models, but these will not concern us in this paper.

- (3) Wino masses enter Eq. (1) only via loop corrections and can be in the 4–5 TeV range without endangering naturalness [35], though in models with gaugino mass unification their mass is somewhat more tightly constrained by the naturalness limit on  $m_{\tilde{g}}$  noted above. In any event, the magnitude of the wino mass parameter is expected to be much larger than  $|\mu|$ . As a result, the lighter neutralinos  $\tilde{\chi}_{1,2}^0$  and the lighter chargino  $\tilde{\chi}_1^\pm$  are expected to be Higgsino-like while the heavier neutralinos  $\tilde{\chi}_{3,4}^0$  and the heavy chargino  $\tilde{\chi}_2^\pm$  are expected to be gauginolike. The upper limits on the wino and bino masses are also important in that they severely limit the splitting between the Higgsinos—a small Higgsino mass gap results in very soft visible debris from the decay of the heavier Higgsinos to the LSP. As a result, Higgsino pair production, in spite of its large production cross section at the LHC, is swamped by SM backgrounds [39]. It has been suggested that Higgsino production in association with a hard QCD jet that leads to monojet plus  $\cancel{E}_T$  events with soft dilepton events from the decay  $\tilde{\chi}_2^0 \rightarrow \tilde{\chi}_1^0 \ell \bar{\ell}$  leads to a viable signal [40–42]. Both ATLAS and CMS have explored this channel but up to now have excluded a sizeable portion of the  $\mu - \Delta m$  plane ( $\Delta m = m_{\tilde{\chi}_2^0} - m_{\tilde{\chi}_1^0}$ ) allowed by naturalness considerations [43,44].
- (4) First and second generation squarks and sleptons with restrictions on intrageneration splittings are only weakly constrained by naturalness. They can range up to  $\mathcal{O}(40)$  TeV without jeopardizing naturalness, greatly ameliorating the SUSY flavor problem [45,46].

As noted above, in the context of natural SUSY considerable effort has been expended on the search for Higgsinos because Higgsino masses are bounded above. There have also been many LHC searches for electroweak gauginos though these have mostly been carried out within the context of simplified models with a binolike LSP. These analyses typically assume that the winolike chargino decays via  $\tilde{\chi}_1^\pm \rightarrow W\tilde{\chi}_1^0$  and the heavier neutralino decays via  $\tilde{\chi}_2^0 \rightarrow Z\tilde{\chi}_1^0$  or  $\tilde{\chi}_2^0 \rightarrow h\tilde{\chi}_1^0$ . They also assume that Higgsinos are too heavy to be produced at the LHC.<sup>2</sup> The signals with the lowest backgrounds come from the leptonic decays of the vector bosons and lead to trilepton events + $\cancel{E}_T$  events with hadronic activity only from QCD

radiation, and lead to a lower limit on the wino mass  $\sim 650$  GeV assuming a light LSP [48]. In the model where the chargino decays via  $\tilde{\chi}_1^\pm \rightarrow W(\rightarrow \ell)\tilde{\chi}_1^0$  while the neutralino decays via  $\tilde{\chi}_2^0 \rightarrow h(\rightarrow b\bar{b})\tilde{\chi}_1^0$ , the wino limit extends to about 750–800 GeV for a light LSP [49]. Remarkably, the strongest limits on the wino mass arise from the *hadronic* decays of the  $W$ ,  $Z$ , and  $h$  bosons, and excludes winos lighter than  $\sim 1$  TeV for a bino LSP as heavy as 300 GeV [15,17].

In this paper, we examine the reach of the HL-LHC for winos in the context of natural SUSY.<sup>3</sup> These winos will for the most part decay into the lighter Higgsinos plus a  $W$ ,  $Z$ , or  $h$ , with branching fractions in the ratio 2:1:1. Our focus will be on the wino states  $\tilde{\chi}_2^\pm$  and  $\tilde{\chi}_4^0$  because the binolike  $\tilde{\chi}_3^0$  couples to gauge bosons (we assume that squarks are very heavy) only via mixing.<sup>4</sup> As already noted in Ref. [51], wino pair production thus leads to  $VV$ ,  $Vh$ , and  $hh + \cancel{E}_T$  ( $V = W, Z$ ) channels via which to search for SUSY at high energy colliders. Motivated by the ATLAS and CMS analyses, we examine signals from both leptonic as well as hadronic decays of the daughter  $W$  and  $Z$  boson daughters of the winos.

The analysis methods developed in the early days of supersymmetry to search for winos decaying to binos (assuming decoupled Higgsinos) must be adapted for the search for heavy winos of natural SUSY as long as the visible decay products of the daughter Higgsinos are assumed to be too soft for detection. We, of course, need to keep track of the branching fractions of the charged and neutral winos to decay via the  $W$ ,  $Z$ , or  $h$  channels. The cleanest channels—which come from the leptonic decays of the bosons and yield events with up to four hard leptons plus  $\cancel{E}_T$ —were examined in Ref. [52] a decade ago. It should be straightforward for the ATLAS and CMS collaborations to incorporate the branching fractions for wino decays predicted by natural SUSY models and repeat their analyses to obtain wino mass bounds within this presumably more realistic/plausible framework. In the absence of a SUSY signal, this may not seem essential. The situation will be very different if a signal appears in Run 3 or in the HL-LHC run in the future because the model *predicts* relative rates for the signals in various leptonic channels as well as in mixed hadron-lepton channels and purely hadronic channels, with and without  $b$  tags.

The remainder of this paper is organized as follows. In the next section we introduce the nonuniversal Higgs mass

<sup>2</sup>Strictly speaking if  $\tilde{\chi}_2^0$  is winolike and  $\tilde{\chi}_1^0$  is binolike, the decay  $\tilde{\chi}_2^0 \rightarrow h\tilde{\chi}_1^0$  would dominate  $\tilde{\chi}_2^0 \rightarrow \tilde{\chi}_1^0 Z$  because (as explained in Sec. VII), the latter can occur only via the suppressed Higgsino components of *both*  $\tilde{\chi}_1^0$  and  $\tilde{\chi}_2^0$ , while the decay to the Higgs boson requires just a single mixing angle suppression. The importance of the  $W(\rightarrow \ell\nu)h(\rightarrow b\bar{b})$  signal from wino production at the LHC was first pointed out in Ref. [47].

<sup>3</sup>For a survey of chargino and neutralino signals in the  $\mu - M_2$  plane assuming a decoupled bino, see Ref. [50].

<sup>4</sup>For definiteness, we assume gaugino mass unification which makes the bino lighter than the neutral wino in our calculations. In models where the bino is heavier than the wino, our results on wino signals will be qualitatively unaltered (keep in mind that wino decays to the binolike state are suppressed by mixing angles) if we remember to interchange  $\tilde{\chi}_3^0 \leftrightarrow \tilde{\chi}_4^0$ .

model that we use for the analysis of the wino signal in natural SUSY models at the HL-LHC. In Sec. III, we discuss the production cross sections for electroweakino (EWino) production at a  $pp$  collider with  $\sqrt{s} = 14$  TeV. In Sec. IV we map out the decay patterns of EWinos in models with small values of  $|\mu|$ , one of the key characteristics of natural SUSY models. In Sec. V we delineate the various channels and detail the analysis cuts that we use to optimize the search for winos. In Sec. VI, we present our results for the HL-LHC discovery reach for winos in natural SUSY models. In Sec. VII, we discuss whether an examination of the HL-LHC signal from winos by itself can provide evidence for the existence of a Higgsino-like LSP. We end in Sec. VIII with a summary of our results and some general remarks.

## II. A NATURAL SUSY MODEL LINE

For our phenomenological analysis of wino signals, we use the two extra parameter nonuniversal Higgs model (NUHM2) [53–55] specified by parameters

$$m_0, m_{1/2}, A_0, \tan\beta, \mu, m_A.$$

The universal SUSY breaking matter scalar mass parameter,  $m_0$ ; the universal SUSY breaking gaugino mass parameter,  $m_{1/2}$ ; and the universal SUSY breaking trilinear scalar coupling,  $A_0$  are all specified at the grand unified theory (GUT) scale while the remaining three parameters are specified at the weak scale.<sup>5</sup> This form of the NUHM2 parameter space is very convenient for studies of natural SUSY because  $|\mu|$  can be chosen to be in the 100–350 GeV range as required. For our wino analysis we adopt the model line

$$\begin{aligned} m_0 &= 5 \text{ TeV}, m_{1/2}, A_0 = -1.6m_0, \tan\beta = 10, \\ \mu &= 250 \text{ GeV} \quad \text{and} \quad m_A = 2 \text{ TeV}, \end{aligned} \quad (3)$$

which ensures modest values of  $\Delta_{EW}$  along with a value of the light Higgs boson mass  $m_h = 125 \pm 2$  GeV. We have, therefore, dubbed this the  $m_h^{125}(nat)$  scenario. By changing  $m_{1/2}$  we can vary the mass of the wino.

We use the computer code ISAJET [56] which includes Isasugra to obtain the sparticle spectrum and weak scale couplings relevant for phenomenology. A sample spectrum for  $m_{1/2} = 1.2$  TeV which yields  $\Delta_{EW} = 22$  is listed in Table 1 of Ref. [57].

<sup>5</sup>The NUHM2 framework allows for independent soft SUSY breaking Higgs mass parameters  $m_{H_u}^2$  and  $m_{H_d}^2$  at the GUT scale. These have been traded in for the weak scale parameters  $\mu$  and  $m_A$ . The assumed universality of matter scalar mass parameters ameliorates unwanted flavor-changing effects.

We should mention that although we are using the NUHM2 framework with unified gaugino mass parameters, this aspect plays a very little role in our examination of the phenomenology of winos at HL-LHC. We do not look at gluino events, and except for relatively small values of  $m_{1/2}$  where the bino mass parameter is small enough so that mixing with Higgsinos is sizeable, the bino state plays no role in our analysis since matter sfermions are taken to be heavy. For all practical purposes,  $m_{1/2}$  only serves to determine the mass of the wino. Finally, since we make no attempt to look at the soft debris from Higgsino decays, our results should only be mildly sensitive to the choice of  $\mu = 250$  GeV, at least for a wino mass much larger than  $|\mu|$ . For convenience, we note that the weak scale wino mass  $M_2 \sim 0.8m_{1/2}$ .

## III. EWINO PRODUCTION CROSS SECTIONS AT LHC14

We begin by considering the production cross sections for pair production of EWinos at the LHC. For our calculation of the next-to-leading-order (NLO) cross sections, we use the computer program PROSPINO [58] using the masses and mixing angles as given by the ISAJET [56] Les Houches Accord files.

Our results are shown in Fig. 1 for (a) chargino pair production, (b) associated chargino-neutralino production, and (c) neutralino pair production. We display the cross sections versus  $m_{1/2}$  for the  $m_h^{125}(nat)$  model line defined by Eq. (3). The region with  $m_{1/2} \lesssim 1.1$  TeV is excluded at 95% CL by the nonobservation of any excess of events in the wino search at the LHC [15,17].<sup>6</sup>

Higgsino pair production is the dominant EWino production cross section in all the panels with a value at the hundreds of fb level. Since the lighter EWinos  $\tilde{\chi}_1^\pm, \tilde{\chi}_1^0$ , and  $\tilde{\chi}_2^0$  are dominantly Higgsino-like with a mass close to  $|\mu|$  over essentially the entire range of the plot, the cross section shows little variation with  $m_{1/2}$ . Note also that pair production of identical neutralinos is dynamically suppressed. As noted in Sec. I, these Higgsino pair production processes are not directly of interest to us in this paper because the visible decay products from Higgsinos are quite soft causing the Higgsino pair signal to be difficult to extract at the LHC.

The next highest cross sections are for wino pair production processes  $\tilde{\chi}_2^\pm\tilde{\chi}_2^\pm$  and  $\tilde{\chi}_2^\pm\tilde{\chi}_4^0$  in Fig. 1(a) and Fig. 1(b), respectively. Wino pair production occurs via the large  $SU(2)$  gauge coupling and is essentially unsuppressed by mixing angles in natural SUSY models.

<sup>6</sup>There is some slop in the lower limit on  $m_{1/2}$  which has been obtained using simplified model analyses, with different assumptions of the branching ratios for wino decays than in the model adopted in this paper.

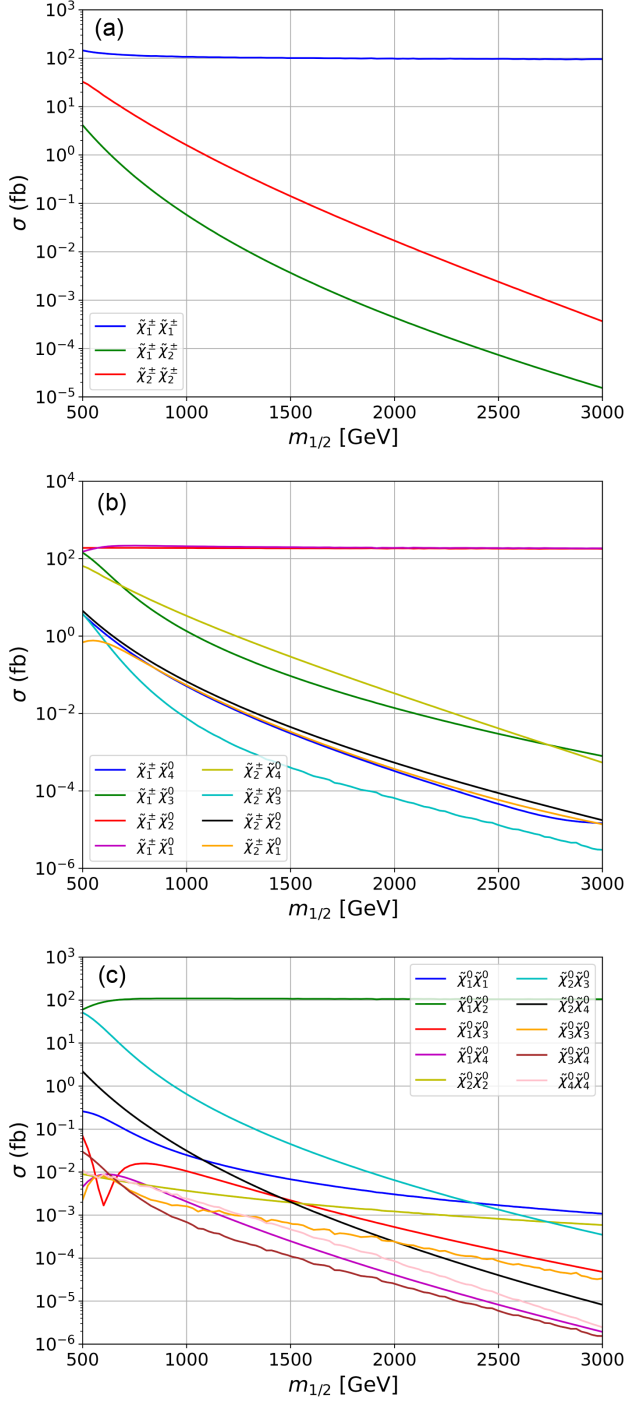


FIG. 1. NLO cross sections for EWino production at a  $pp$  collider with  $\sqrt{s} = 14$  TeV versus  $m_{1/2}$  for the  $m_h^{125}(\text{nat})$  model line introduced in Eq. (3) of the text. We show cross sections for (a) chargino pair production, (b) chargino-neutralino pair production, and (c) neutralino pair production.

These are at the 1 fb level for  $m_{1/2} = 1$  TeV, and, of course, fall with increasing values of  $m_{1/2}$ . However, even for  $m_{1/2}$  as large as 1.8 TeV, we may expect about 100 wino pair events in a sample of  $3000 \text{ fb}^{-1}$ . Neutral wino pairs cannot couple to the  $Z$  boson because of  $SU(2)$  symmetry,

and so the  $\tilde{\chi}_4^0 \tilde{\chi}_4^0$  production in Fig. 1(c) is strongly suppressed. Wino-bino production processes,  $\tilde{\chi}_3^0 \tilde{\chi}_4^0$  and  $\tilde{\chi}_3^\pm \tilde{\chi}_4^\pm$  are also suppressed for reasons already mentioned in Sec. I.

Finally, we turn to gaugino-Higgsino pair production. Since gauge bosons couple only to Higgsino pairs or gaugino pairs, gaugino-Higgsino pair production from  $q\bar{q}$  collisions via virtual  $W$  or  $Z$  exchange in the  $s$  channel is suppressed by the gaugino-Higgsino mixing. As a result, in the model with unified gaugino masses where  $M_2 \simeq 2M_1$ , wino-Higgsino mixing is smaller than bino-Higgsino mixing. Thus the various wino-Higgsino processes in the Fig. 1 are suppressed relative to the corresponding bino-Higgsino processes, both by kinematic ( $M_2 > M_1$ ) as well as dynamical reasons (e.g.,  $\tilde{\chi}_1^\pm \tilde{\chi}_3^0$  vs  $\tilde{\chi}_1^\pm \tilde{\chi}_4^0$  or  $\tilde{\chi}_2^0 \tilde{\chi}_3^0$  vs  $\tilde{\chi}_2^0 \tilde{\chi}_4^0$ ). Indeed, the cross sections in Fig. 1 for some of the bino-Higgsino processes, such as  $\tilde{\chi}_3^0 \tilde{\chi}_1^\pm$  production in frame (b) or  $\tilde{\chi}_3^0 \tilde{\chi}_2^0$  in frame (c) are comparable in magnitude to the cross section for the wino pair [ $\tilde{\chi}_2^\pm \tilde{\chi}_2^\pm$  production in frame (a) or  $\tilde{\chi}_2^\pm \tilde{\chi}_4^0$  production in frame (b)] whose LHC signatures are the subject of this paper.

#### IV. ELECTROWEAK GAUGINO BRANCHING FRACTIONS IN NATURAL SUSY

LHC signatures for wino production depend on how these decay. The branching fractions, within natural SUSY, for decays of the charged and the neutral winolike states are shown versus  $m_{1/2}$  in Figs. 2(a) and 2(b), respectively. We obtain the branching fractions from ISAJET. As in Fig. 1, the other parameters are fixed by Eq. (3). We see that for  $m_{1/2} \gtrsim 1$  TeV where phase space effects are unimportant for the analysis of wino decays,  $B(\tilde{\chi}_2^\pm \rightarrow W\tilde{\chi}_{1,2}^0) : B(\tilde{\chi}_2^\pm \rightarrow h\tilde{\chi}_1^\pm) : B(\tilde{\chi}_2^\pm \rightarrow Z\tilde{\chi}_1^\pm) \simeq 2:1:1$ , with a very small fraction of the  $\tilde{\chi}_2^\pm$  decaying via the dynamically and kinematically suppressed decay to the bino. Here, we sum over the decays to the neutral Higgsinos since as mentioned previously, we do not attempt to identify the soft visible decay products of the Higgsinos. Likewise, from Fig. 2(b) we see that even for neutral winos,  $B(\tilde{\chi}_4^0 \rightarrow W^\mp \tilde{\chi}_1^\pm) : B(\tilde{\chi}_4^0 \rightarrow h\tilde{\chi}_{1,2}^0) : B(\tilde{\chi}_4^0 \rightarrow Z\tilde{\chi}_{1,2}^0) = 2:1:1$  as long as these are heavy, while the decay to the bino is again strongly suppressed. The reason for this simple 2:1:1 pattern of charged and neutral branching ratios has been explained in Ref. [59], and we will not repeat it here.

Although not germane to the considerations of this paper, for completeness we show the branching fractions for the *two-body decays* of the binolike  $\tilde{\chi}_3^0$  state in Fig. 2(c). For small values of  $m_{1/2}$  in the left-most part of the panel, the  $\tilde{\chi}_3^0$  is too light to decay to Higgsinos together with an on shell vector boson, and so decays via three-body modes. The first two-body modes to become accessible are  $\tilde{\chi}_3^0 \rightarrow \tilde{\chi}_1^0 Z$  and  $\tilde{\chi}_3^0 \rightarrow \tilde{\chi}_1^\pm W$ . Indeed in the region where  $m_{1/2} \sim 700\text{--}800$  GeV where the two-body

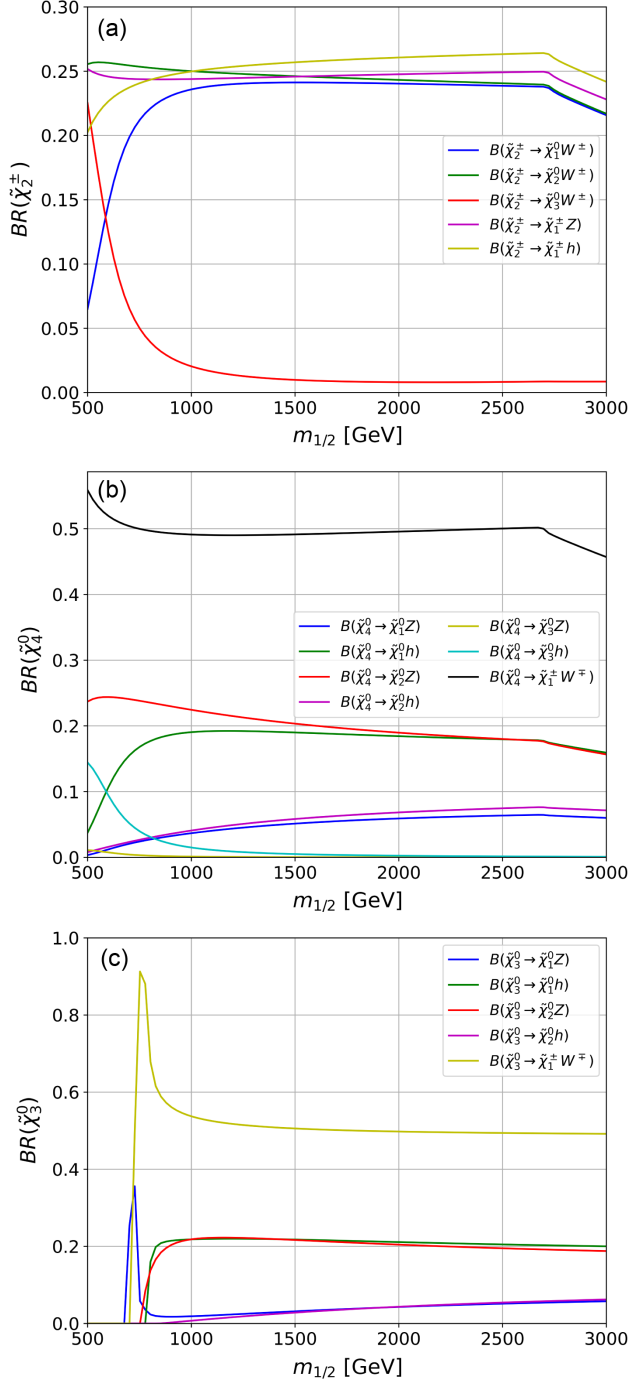


FIG. 2. Branching fractions from natural SUSY versus  $m_{1/2}$  for the model line defined by Eq. (3) for (a) the charged winolike state,  $\tilde{\chi}_2^\pm$ , (b) the neutral winolike state,  $\tilde{\chi}_4^0$ , and (c) the binolike state  $\tilde{\chi}_3^0$ . We show the branching fractions only for two-body decay channels, all of which are closed for small values of  $m_{1/2}$  in (c).

decays turn on,  $M_1$  is comparable to  $\mu$ , and the lighter states are well-mixed binos and Higgsinos, with only the heaviest states being winolike. For values of  $m_{1/2}$  larger than  $\sim 0.9\text{--}1$  TeV, our expectation is that the mass

eigenstates are dominantly Higgsino-, bino-, or winolike, and we see once again the simple 2:1:1 decay pattern for decays to  $W$ ,  $Z$  and  $h$  bosons, for more or less the same reason as for the decay of the neutral wino states [59].

## V. WINO DISCOVERY CHANNELS

We now turn our attention to the potential of HL-LHC ( $\sqrt{s} = 14$  TeV with  $3000 \text{ fb}^{-1}$ ) for probing wino pair production in the context of natural SUSY. We use ISAJET to first construct a SUSY Les Houches Accord file [60] for any natural SUSY parameter-space point and feed this into PYTHIA [61] to generate signal events. We also use PYTHIA to generate the various  $2 \rightarrow 2$  background processes. For  $2 \rightarrow 3$  background processes, we use MadGraph [62], coupled with PYTHIA. For our computation of SM backgrounds to the gaugino signal, we include parton level production of  $t\bar{t}$ ,  $t\bar{t}V$ ,  $h\bar{t}t$ ,  $hh$ ,  $hhV$ ,  $V + \text{jets}$ ,  $Vh$ ,  $VV$ , and  $VVV$  final states to evaluate SM backgrounds. Specifically, we normalize the SUSY cross sections to their NLO values obtained from Prospino. For the most important SM backgrounds we normalize the cross sections to their values at the NLO level, or better when available. The NNLO (next-to-next-to-leading-order)/NNLL (next-to-next-to-leading-log)  $t\bar{t}$  cross section is normalized to  $985.7 \text{ pb}$ ,<sup>7</sup> the cross sections for  $t\bar{t}V$  production are from Ref. [63],  $V + j$  and  $Vb\bar{b}$  cross sections are calculated using the  $K$ -factor from the ratio of NLO and leading order (LO) cross sections from MadGraph with parton jets defined using the anti- $k_T$  algorithm with  $p_{Tj} > 25 \text{ GeV}$  and  $\Delta R = 0.4$ , and finally  $VV$  cross sections are normalized using the results in Ref. [64]. The remaining backgrounds which are frequently orders of magnitude smaller are included at leading order. We use the DELPHES code for detector simulation in our analysis [65].

Since our signal consists of combinations of high transverse momentum  $W$ ,  $Z$ , and  $h$  bosons decaying leptonically or hadronically, we focus on hard leptons and jets in the central part of the detector. With this in mind, we require isolated electrons and muons to satisfy

- (1)  $p_T(e) > 20 \text{ GeV}$ ,  $|\eta_e| < 2.47$ , with  $P_{T\text{Ratio}} < 0.1$ , and
- (2)  $p_T(\mu) > 25 \text{ GeV}$ ,  $|\eta_\mu| < 2.5$  with  $p_{T\text{Ratio}} < 0.2$ ,

where  $P_{T\text{Ratio}}$  is defined as the ratio of the scalar sum of the transverse momentum of objects (defined in the default DELPHES configuration card for HL-LHC simulation) in a  $\Delta R = 0.3$  cone about the lepton.

We construct small radius (SR) jets using an anti- $k_T$  jet algorithm and require

<sup>7</sup>This is taken from <https://twiki.cern.ch/twiki/bin/view/LHCPhysics/TtbarNNLO> where references to the literature for the calculation may also be found.

- (1)  $p_T(SRj) > 25$  GeV with a cone size  $R \leq 0.4$  and  $|\eta(SRj)| < 4.5$ .

The jet is labeled as a  $b$  jet if, in addition, it satisfies

- (1)  $|\eta_j| < 2.4$  and is tagged as a  $b$  jet by DELPHES.

Since our aim is to also identify hadronically decaying high  $p_T$  gauge and Higgs bosons,<sup>8</sup> we construct large radius (LR) jets using an anti- $k_T$  jet algorithm with a cone  $R < 1.5$ , and require

- (1)  $p_T(LRj) > 300$  GeV and  $\eta(LRj) < 2$ .

We use the identified leptons, SR jets, and LR jets to construct  $W, Z$  and  $h$  candidates as follows.

*Leptonically decaying Z:*

A pair of opposite sign (OS) leptons with the same flavor (SF) satisfying  $80$  GeV  $< m(\ell\ell) < 100$  GeV is identified as a candidate  $Z$  boson.

*Hadronically decaying W:*

A LR jet with trimmed mass [66]  $60$  GeV  $< m_J < 90$  GeV is identified as a candidate  $W$  boson.

*Hadronically decaying Z:*

Either (or both)

- (a) two small radius signal  $b$  jets that have an invariant mass  $80$  GeV  $< m(bb) < 100$  GeV,

or

(b) a LR jet with trimmed mass  $70$  GeV  $< m_J < 100$  GeV defines a candidate  $Z$  boson. We do not attempt to distinguish between LR jets from  $W$  and  $Z$  bosons, but simply classify LR jets with a trimmed mass between  $60$  GeV  $< m_J < 100$  GeV as a vector boson.

*Higgs bosons:*

Either (or both)

- (a) two small radius signal  $b$  jets that have an invariant mass  $100$  GeV  $< m(bb) < 135$  GeV,

or

- (b) LR jet with trimmed mass  $100$  GeV  $< m_J < 135$  GeV, and at least one small radius ( $R < 0.4$ ) signal  $b$  jet within the cone radius of the LR jet

define a candidate SM-like Higgs boson,  $h$ .

Having discussed how we identify candidate hadronically decaying  $W, Z$ , and  $h$  daughters of winos (these have the largest branching fractions and so lead to the largest

signal rates) we proceed to classify events into eight channels:

- (1)  $Z(\rightarrow \ell^+\ell^-)B + \cancel{E}_T$ ,
- (2)  $h/Z(\rightarrow bb)B + \cancel{E}_T$ ,
- (3)  $BB + \cancel{E}_T$ ,
- (4)  $\ell h + \cancel{E}_T$ ,
- (5)  $\ell B_{W/Z} + \cancel{E}_T$ ,
- (6)  $Z(\rightarrow \ell^+\ell^-) + \cancel{E}_T$ ,
- (7)  $h/Z(\rightarrow bb) + \cancel{E}_T$ , and
- (8)  $\ell^\pm\ell^\pm + \cancel{E}_T$  events from  $q\bar{q} \rightarrow \tilde{W}^\pm(\rightarrow W^\pm\tilde{h}^0)\tilde{W}^0(\rightarrow W^\pm\tilde{h}^\mp)$ , where the  $W$  bosons decay leptonically and the decay products of Higgsinos are soft so that these events have hadronic activity only from QCD radiation [59,67].

Here,  $B$  (for boson) means any hadronically decayed  $W, Z$ , or  $h$  boson as defined above, while  $B_{W/Z}$  refers to hadronically decaying  $W$  and  $Z$  bosons identified as LR jets with  $60$  GeV  $< m_J < 100$  GeV. It may appear that the same event may be classified in more than one channel; e.g., an event with a Higgs boson  $h \rightarrow bb$  produced in association with a hadronically decaying  $W$  may be classified in both the  $h/Z(\rightarrow bb)B + \cancel{E}_T$  as well as the  $BB + \cancel{E}_T$  channels. We have ensured this is not the case. If an event satisfies the criteria in more than one channel, we classify it to be in the channel that appears first on the list, and do not count it again in any of the subsequent channels. The fact that these channels are nonoverlapping will be important when we combine them to project the significance of the signal. These channels are defined as follows.

- (1)  $Z(\rightarrow \ell^+\ell^-)B + \cancel{E}_T$ :
  - (a) Exactly one pair of OS/SF leptons.
  - (b)  $80$  GeV  $< m(\ell\ell) < 100$  GeV.
  - (c) One hadronically decayed  $W/Z/h$ .
  - (d) If the hadronically decayed  $W/Z/h$  is tagged with a LR jet, the two leptons should be outside the cone radius of this LR jet  $\Delta R(J, \ell) > 1.5$ .
- (2)  $h/Z(\rightarrow bb)B + \cancel{E}_T$ : Events that fail the previous classification criterion, but satisfy
  - (a) No isolated leptons.
  - (b) At least two  $b$  jets.
  - (c) At least one pair of  $b$  jets has an invariant mass of  $80$  GeV  $< m(bb) < 135$  GeV.
  - (d) Besides the  $b$  pair that reconstructs  $h/Z$ , one other hadronically decayed  $W/Z/h$ .
  - (e) If the hadronically decaying boson is tagged with a LR jet, the two  $b$  jets that reconstruct  $h/Z$  should be outside the cone radius of the LR jet  $\Delta R(J, b) > 1.5$ , with no other  $b$  jets allowed outside the cone radius of the LR jet.
- (3)  $BB + \cancel{E}_T$ : Events that fail all the above classification criteria, but contain
  - (a) Two hadronically decayed  $W/Z/h$ , each being tagged with a LR jet.
- (4)  $\ell h + \cancel{E}_T$ : Events that fail all the above classification criteria, but contain

<sup>8</sup>The analyses of electroweak gaugino signals at hadron colliders before the LHC focused on the leptonic decays of the gauginos because backgrounds to the hadronic signals were thought to be large. Subsequent developments in our understanding of jet substructure now allow us to zero in on the signal from hadronic decays of boosted, heavy daughters of heavy gauginos without being completely overwhelmed by QCD radiation. Gaugino searches at even the Tevatron were confined to gaugino mass ranges where the gaugino decayed via three-body decays, or where the daughter bosons from gaugino decay were not particularly boosted. An additional factor that may have precluded earlier exploration of hadronic decays of gauginos is that the magnitude of  $\cancel{E}_T$  from hadronic mismeasurements scales as a square root of the total scalar  $E_T$  in the event, and so is fractionally less relevant compared to the physics  $\cancel{E}_T$  at higher masses probed at the LHC.

- (a) at least one isolated lepton<sup>9</sup>;
  - (b) exactly one Higgs boson  $h$ ;
  - (c) if the Higgs is tagged with a LR jet, the lepton candidates should be outside the cone radius of this LR jet  $\Delta R(J, \ell) > 1.5$ ; and
  - (d) if there are two or more lepton candidates, the one that minimizes the magnitude of  $\vec{E}_T + \vec{p}_T(h) + \vec{p}_T(\ell)$  is chosen as the lepton.
- (5)  $\ell B_{W/Z} + \cancel{E}_T$ : Events that fail all the above classification criteria, but contain
- (a) at least one isolated lepton;
  - (b) exactly one hadronically decaying  $W/Z$  boson tagged as a LR jet;
  - (c) the lepton candidates should be outside the cone radius of the signal LR jet  $\Delta R(J, \ell) > 1.5$ ; and
  - (d) if there are two or more lepton candidates, the one that minimizes the magnitude of  $\vec{E}_T + \vec{p}_T(W/Z) + \vec{p}_T(\ell)$  is chosen as the lepton.
- (6)  $Z(\rightarrow \ell^+ \ell^-) + \cancel{E}_T$ : Events that fail all the above classification criteria, but contain
- (a) exactly one pair of OS/SF leptons; and
  - (b)  $80 \text{ GeV} < m(\ell\ell) < 100 \text{ GeV}$ .
- (7)  $h/Z(\rightarrow bb) + \cancel{E}_T$ : Events that fail all the above classification criteria, but contain
- (a) at least two  $b$  jets; and
  - (b) exactly one pair of  $b$  jets has an invariant mass of  $80 \text{ GeV} < m(bb) < 135 \text{ GeV}$ .
- (8)  $\ell^\pm \ell^\pm + \cancel{E}_T$ : Events that fail all the above classification criteria but contain
- (a) exactly two same-sign leptons with large  $\cancel{E}_T$ ; and
  - (b) no tagged  $b$  jets.

Having decided on the various channels for the wino search, we now proceed with the analysis of the signal in each of these channels. Toward this end, we have examined several signal and SM background distributions to develop analysis cuts that serve to enhance the gaugino signal in each of the eight channels. We do not show these distributions here; instead, we only display the additional channel-by-channel cuts that we use to assess the observability of the gaugino signal over SM backgrounds. For each channel with two tagged bosons (including the  $\ell h + \cancel{E}_T$  and  $\ell B_{W/Z} + \cancel{E}_T$  channels) we show  $m_{T2}$  [68] distributions after analysis cuts, while for the channels with just a single tagged boson we show corresponding  $m_T$  distributions that we use for subsequent statistical analysis of the observability of the signal. For the same-sign dilepton plus  $\cancel{E}_T$  channel, we show instead the distribution of  $L_T \equiv |p_T(\ell_1)| + |p_T(\ell_2)| + |\cancel{E}_T|$ . Our goal is to examine

<sup>9</sup>We found requiring at least one isolated lepton proved better than exactly one isolated lepton because  $\sim 10\%$  of signal events contained additional leptons, presumably from the decays of the daughter Higgsinos.

whether these distributions are significantly modified from SM expectation due to the presence of a signal.

### A. $Z(\rightarrow \ell^+ \ell^-)B + \cancel{E}_T$ channel

We begin our investigation with the  $Z(\rightarrow \ell^+ \ell^-)B + \cancel{E}_T$  channel. Upon analyzing various kinematics distributions, we require additional analysis cuts:

- (1)  $\cancel{E}_T > 350 \text{ GeV}$ ;
- (2)  $\max[m_T(Z(\ell^+ \ell^-), \cancel{E}_T), m_T(B, \cancel{E}_T)] > 1000 \text{ GeV}$ ;
- (3)  $\min[m_T(b, \cancel{E}_T)] > 175 \text{ GeV}$ , where  $b$  loops over all  $b$  jets;
- (4)  $\Delta R(\ell^+, \ell^-) < 0.8$ ; and
- (5)  $\min[\Delta\phi(J, \cancel{E}_T)] > 35^\circ$ , where  $J$  loops over all LR jets in the event, no matter whether these have been tagged as a boson or not.

The  $m_{T2}$  distribution, after these cuts, is shown in Fig. 3 for both the signal as well as for the leading SM backgrounds. We show the signal histograms for  $m_{1/2} = 1.3$  and  $1.6 \text{ TeV}$  (corresponding to a charged wino mass of  $1.1$  and  $1.35 \text{ TeV}$ , respectively) along the model line defined by Eq. (3). The primary backgrounds are depicted by the filled histograms and mainly come from  $WZ$  and  $ZZ$  production. The lower  $m_{T2}$  region is dominated by the background. The signal begins to emerge from the background at increased  $m_{T2}$  values determined by the parent gaugino masses until it cuts off at high values of  $m_{T2}$ . Our goal is to examine whether the wino signal sufficiently distorts the expectation of the event rate from SM expectation so that one can claim a discovery of new physics for the chosen value of  $m_{1/2}$  after combining (see Sec. VI below) the eight different channels

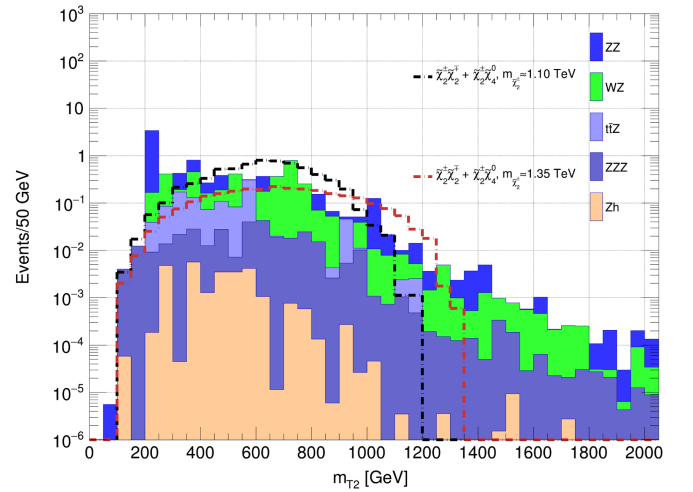


FIG. 3. The distribution of  $m_{T2}(Z(\ell^+ \ell^-)B, E_T)$  after the analysis cuts detailed in the text for the wino signal for  $m_{1/2} = 1.3$  and  $1.6 \text{ TeV}$ , with other parameters fixed as in Eq. (3) is shown by the hollow histograms. The corresponding background distributions are shown by the filled histograms. The background histograms are not stacked.

that we analyze. If instead the signal is too small to cause a sufficient deviation from SM expectations, the corresponding value of  $m_{1/2}$  can be excluded.

### B. $h/Z(\rightarrow bb)B + \cancel{E}_T$ channel

For wino searches via this channel, after analyzing various distributions, we require additional analysis cuts:

- (1)  $\cancel{E}_T > 450$  GeV;
- (2) No jet in the event is tagged as  $\tau$  by DELPHES;
- (3)  $\max[m_T(h/Z(bb), \cancel{E}_T), m_T(B, \cancel{E}_T)] > 1100$  GeV;
- (4)  $\min[m_T(b, \cancel{E}_T)] > 175$  GeV, where  $b$  loops over all  $b$  jets;
- (5)  $\min[\Delta\phi(J, \cancel{E}_T)] > 35^\circ$ , where  $J$  loops over all LR jets in the event, whether or not these have been tagged as a  $W$ ,  $Z$  or  $h$  boson; and
- (6) No LR jets in the event should have a trimmed mass in the mass range of top, so  $m_J \notin (135, 185)$  GeV.

The resulting  $m_{T2}$  distributions are displayed in Fig. 4 for both the two signal cases (hollow histograms) shown in the last figure as well as leading SM backgrounds (solid histograms). In this channel, the largest backgrounds are from  $t\bar{t}$  and  $Z + b\bar{b}$  production. Once again, we see that the signal distributions have broad peaks and cut off at  $m_{T2}$  values determined by the wino mass, while the background is largely a broad continuum. The signal histograms distinctly rise above the background at large  $m_{T2}$  values before their kinematic cutoff.

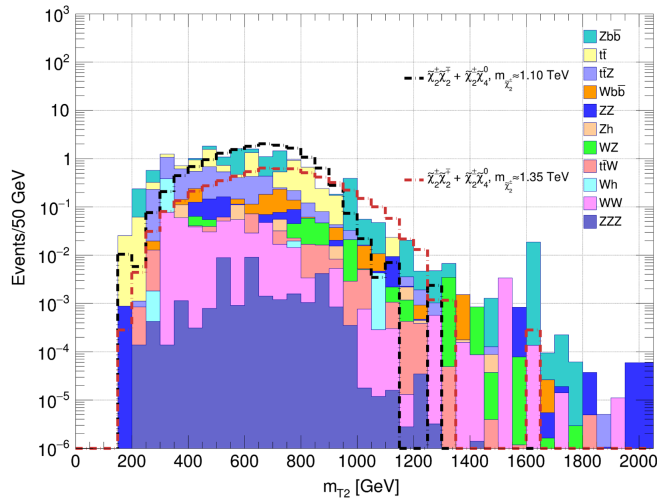


FIG. 4. The distribution of  $m_{T2}(h/Z(bb)B, E_T)$  after the analysis cuts detailed in the text for the wino signal for  $m_{1/2} = 1.3$  and  $1.6$  TeV, with other parameters fixed as in Eq. (3) is shown by the hollow histograms. The corresponding background distributions are shown by the filled histograms. The background histograms are not stacked.

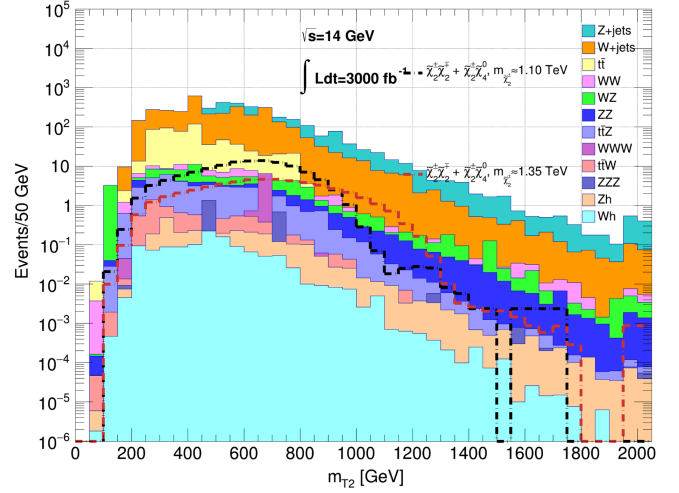


FIG. 5. The distribution of  $m_{T2}(BB, E_T)$  after the analysis cuts detailed in the text for the wino signal for  $m_{1/2} = 1.3$  and  $1.6$  TeV, with other parameters fixed as in Eq. (3) is shown by the hollow histograms. The corresponding background distributions are shown by the filled histograms. The background histograms are not stacked.

### C. $BB + \cancel{E}_T$ channel

Next, we examined various distributions for signal and background in the  $BB + \cancel{E}_T$  channel to arrive at the following analysis cuts:

- (1)  $\cancel{E}_T > 200$  GeV;
- (2) No jet in the event is tagged as  $\tau$  by DELPHES;
- (3)  $\max[m_T(B_1, \cancel{E}_T), m_T(B_2, \cancel{E}_T)] > 1000$  GeV;
- (4)  $\min[m_T(b, \cancel{E}_T)] > 175$  GeV, where  $b$  loops over all  $b$  jets;
- (5)  $\min[\Delta\phi(J, \cancel{E}_T)] > 35^\circ$ , where  $J$  loops over all LR jets in the event whether they have been tagged as a boson; and
- (6) No LR jet in the event should have a trimmed mass in the mass range of top, so  $m_J \notin (135, 185)$  GeV.

The resulting signal and background  $m_{T2}$  distributions are shown in Fig. 5, again for the same signal cases as before. As in previous figures, the signal distribution is bounded above by the wino mass. In this channel,<sup>10</sup> however, the enormous  $W/Z + \text{jets}$  and also the  $t\bar{t}$  backgrounds completely overwhelm the signal even after selection cuts. We might think that this channel will make a negligible contribution to the significance of the wino signal at the HL-LHC. Notice, however, that the signal cross sections as well as the backgrounds in this channel are an order of magnitude larger than for other channels discussed, so that the naive measure “ $S/\sqrt{B}$ ” (over a few optimally chosen bins) might make this channel competitive. Systematic uncertainties may change this picture though.

<sup>10</sup>Bear in mind that  $Z(\rightarrow \ell\bar{\ell})B + E_T$  events and  $h/Z(\rightarrow bb)B + E_T$  events which have been included in previous channels are not counted in this channel.

### D. $\ell^\pm h + \cancel{E}_T$ channel

In this channel our intent is to target events where one of the winos decays into a leptonically decaying  $W$  boson, while the other wino decays to the light Higgs boson. After examining various distributions we further require the following:

- (1)  $\cancel{E}_T > 450$  GeV;
- (2) No jet in the event is tagged as  $\tau$  by DELPHES;
- (3)  $\max[m_T(\ell, \cancel{E}_T), m_T(h, \cancel{E}_T)] > 1100$  GeV;
- (4)  $\min[m_T(b, \cancel{E}_T)] > 175$  GeV, where  $b$  loops over all  $b$  jets;
- (5)  $\Delta\phi(h, \cancel{E}_T) > 115^\circ$ ;
- (6)  $\min[\Delta\phi(J, \cancel{E}_T)] > 65^\circ$ , where  $J$  loops over all LR jets in the event, whether or not these have been tagged as a boson; and
- (7) No LR jets in the event should have a trimmed mass in the mass range of top, so  $m_J \notin (135, 185)$  GeV.

The  $m_{T2}$  distributions after these cuts are then shown in Fig. 6 for the two signal cases as well as for various SM backgrounds. SM processes involving  $W$  boson production, either directly from  $VV$  pair production or from decays of top quarks, constitute the dominant backgrounds. The signal distributions are again clearly bounded by the wino mass. Somewhat surprising is the long background tail from SM  $WW$  production because the LR jet from the hadronic decay of the  $W$  boson would not be expected to have the trimmed mass in the 100–135 GeV range, or for that matter include a SR  $b$  jet. However,  $b$  quarks from QCD radiation (or jets mistagged as a  $b$ ) could combine with either a tau jet or hadronic decay products of the  $W$  that are *not* the parent of the lepton to push the LR jet mass

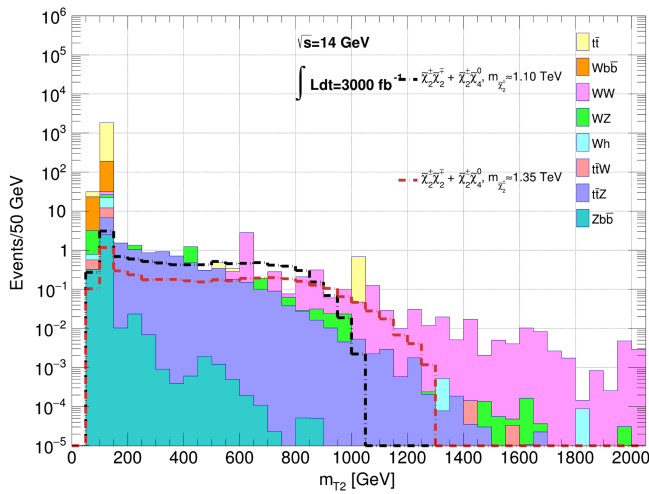


FIG. 6. The distribution of  $m_{T2}(\ell h, E_T)$  after the analysis cuts detailed in the text for the wino signal for  $m_{1/2} = 1.3$  and 1.6 TeV, with other parameters fixed as in Eq. (3) is shown by the hollow histograms. The corresponding background distributions are shown by the filled histograms. The background histograms are not stacked.

into the higher range, causing it to be tagged as an  $h$ . The signal cross sections are comparable in magnitude to the background cross sections, and we may anticipate that this channel will contribute to the significance of the signal at the HL-LHC.

### E. $\ell B_{W/Z} + \cancel{E}_T$ channel

This channel is designed to examine events where one wino decays into a leptonically decaying  $W$  boson and the other decays into a hadronically decaying  $W/Z$  boson tagged as a LR jet, but not a  $Z$  boson tagged via two  $b$  jets reconstructing the  $Z$ . Upon examination of various distributions, we further require the following:

- (1)  $\cancel{E}_T > 500$  GeV;
- (2) No jet in the event is tagged as  $\tau$  by DELPHES;
- (3)  $\max[m_T(\ell, \cancel{E}_T), m_T(B_{W/Z}, \cancel{E}_T)] > 1000$  GeV;
- (4)  $\min[m_T(b, \cancel{E}_T)] > 175$  GeV, where  $b$  loops over all  $b$ -jets;
- (5)  $\Delta\phi(B_{W/Z}, \cancel{E}_T) > 105^\circ$ ; and
- (6)  $\min[\Delta\phi(J, \cancel{E}_T)] > 15^\circ$ , where  $J$  loops over all LR jets in the event, whether or not these have been tagged as a boson.

The  $m_{T2}$  distributions for the two signal cases as well as for various SM backgrounds are shown in Fig. 7. As may have been anticipated, SM processes involving  $WW$  and  $WZ$  pair production are the dominant background source except for the smallest values of  $m_{T2}$  where  $Wj$  production dominates. While the distribution of events from  $WW$  and  $WZ$  production do exhibit a peak at  $m_{T2} \lesssim 100$ –150 GeV, the long tail extending to TeV values of  $m_{T2}$  where we expect the signal to reside may seem somewhat surprising.

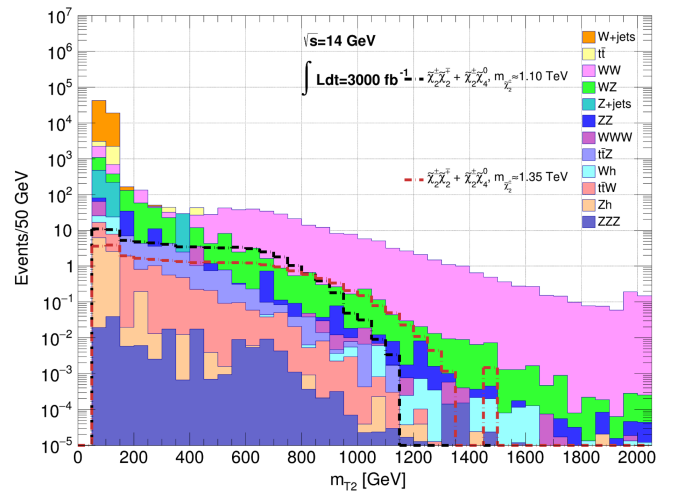


FIG. 7. The distribution of  $m_{T2}(\ell B_{W/Z}, E_T)$  after the analysis cuts detailed in the text for the wino signal for  $m_{1/2} = 1.3$  and 1.6 TeV, with other parameters fixed as in Eq. (3) is shown by the hollow histograms. The corresponding background distributions are shown by the filled histograms. The background histograms are not stacked.

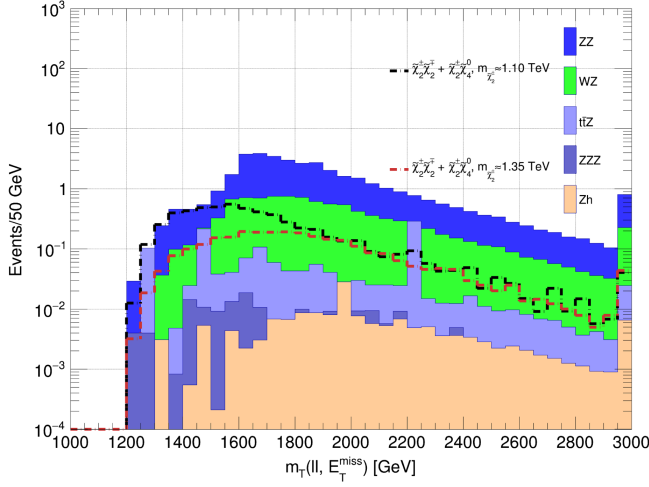


FIG. 8. The distribution of  $m_T(\ell^+\ell^-, E_T)$  after the analysis cuts detailed in the text for the wino signal for  $m_{1/2} = 1.3$  and 1.6 TeV, with other parameters fixed as in Eq. (3) is shown by the hollow histograms. The corresponding background distributions are shown by the filled histograms. The background histograms are not stacked.

We have checked that events with  $m_T(\ell, \cancel{E}_T) < 100$  GeV are essentially all in the low  $m_{T2}$  peak so that imposing a cut on this does not allow the signal to stand out above the long tail in the  $WW$  background.<sup>11</sup> We have further checked that in most of the events in the tail that contain two neutrinos, the second neutrino (for the most part) coming from  $W \rightarrow \tau\nu$  or from  $W \rightarrow s\nu$  decays. The long tail presumably comes from the fact that hard QCD radiation forms part of the LR jet, i.e., the  $B$  is not entirely composed of the decay products of the second  $W$ . As in the  $BB + \cancel{E}_T$  channel studied above, it appears that the backgrounds are one and a half orders of magnitude higher than the signal, but bear in mind that the signal event rate is also higher than in many of the channels where signal and background were comparable in a range of mass bins.

### F. $Z(\rightarrow \ell^+\ell^-) + \cancel{E}_T$ channel

This channel is designed to catch events where both winos decay to a  $Z$  boson, one of which decays leptonically, and the other invisibly to neutrinos. One expects enormous  $\cancel{E}_T$  in these events. After exploring several distributions, we further require the following:

- (1)  $\cancel{E}_T > 750$  GeV;
- (2)  $L_T > 1550$  GeV, where  $L_T$  is defined to be the scalar sum of the  $p_T$  of all jets and leptons, and  $\cancel{E}_T$  in the event; and

<sup>11</sup>Events where one  $W$  decays leptonically and the other boson decays hadronically would be expected to satisfy  $m_T(\ell, E_T) < 100$  GeV if the single neutrino from the leptonic decay of  $W$  is the primary source of  $E_T$ .

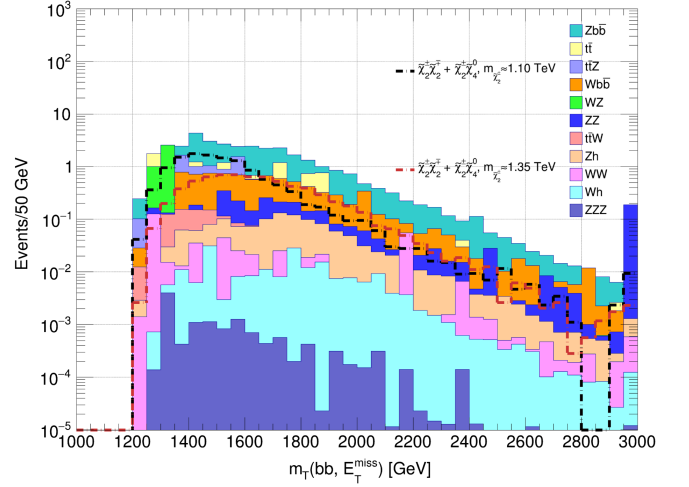


FIG. 9. The distribution of  $m_T(bb, E_T)$  after the analysis cuts detailed in the text for the wino signal for  $m_{1/2} = 1.3$  and 1.6 TeV, with other parameters fixed as in Eq. (3) is shown by the hollow histograms. The corresponding background distributions are shown by the filled histograms. The background histograms are not stacked.

$$(3) \quad \frac{m_{CT} > 100 \text{ GeV}, \quad \text{where} \quad m_{CT} = \sqrt{2p_T(\ell^+)p_T(\ell^-)(1 + \cos(\Delta\phi(\ell^+, \ell^-)))}.$$

Since only one boson is reconstructed in this channel, we show the distribution of cluster transverse mass [69]  $m_T(\ell^+\ell^-, \cancel{E}_T)$  for this channel in Fig. 8 for the two signal cases and for various SM backgrounds. Not surprisingly,  $Z(\rightarrow \ell^+\ell^-)Z(\rightarrow \nu\bar{\nu})$  dominates the SM background followed by  $Z(\rightarrow \ell^+\ell^-)W$  production where the  $W$  decays to an  $e, \mu,$  or  $\tau$  that is missed in the detector. Although the backgrounds are large for  $m_T \gtrsim 1.5$  TeV, the backgrounds are comparable to the wino signal over a significant range, and it seems possible that a distortion of this distribution due to the presence of a signal may contribute to its overall significance when the various channels are combined.

### G. $h/Z(\rightarrow 2b) + \cancel{E}_T$ channel

This channel is designed to catch events where one wino decays to an  $h$  or  $Z$  boson tagged by two SR  $b$  jets with an invariant mass consistent with  $m_Z$  or  $m_h$ , and the other wino decays to a  $Z$  that is essentially invisible. There would, of course, be contributions to this channel where the boson on the other side fails to be tagged, e.g., it is a  $W$  decaying via  $W \rightarrow \tau\nu$ , and the hadronically decaying tau is not identified.

For this channel, we require

- (1)  $\cancel{E}_T > 850$  GeV,
- (2) No jet in the event is tagged as  $\tau$  by DELPHES,
- (3)  $\min[m_T(b, \cancel{E}_T)] > 175$  GeV, where  $b$  loops over all  $b$  jets,

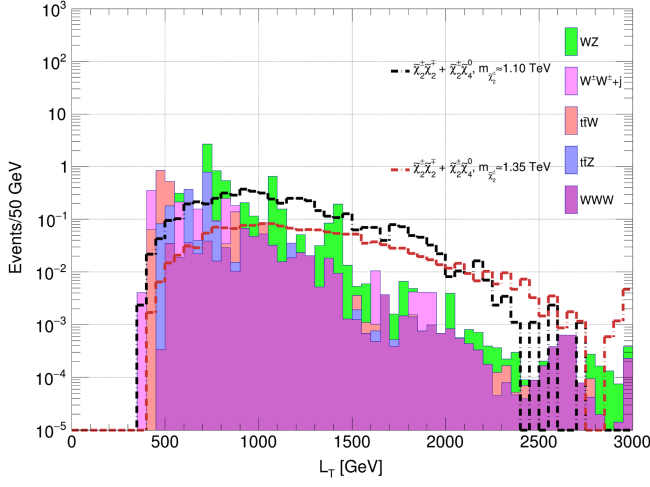


FIG. 10. The distribution of  $L_T \equiv |p_T(\ell_1)| + |p_T(\ell_2)| + |\cancel{E}_T|$  after the analysis cuts detailed in the text for the wino signal for  $m_{1/2} = 1.3$  and 1.6 TeV, with other parameters fixed as in Eq. (3) is shown by the hollow histograms. The corresponding background distributions are shown by the filled histograms. The background histograms are not stacked.

- (4)  $\min[\Delta\phi(b, \cancel{E}_T)] > 85^\circ$ , where  $b$  loops over all  $b$  jets, and
- (5) No LR jets in the event should have a trimmed mass in the mass range of top, so  $m_J \notin (135, 185)$  GeV.

Again, since only one boson is constructed in this channel, we show the distributions of the transverse mass  $m_T(bb, \cancel{E}_T)$  in Fig. 9 for the two signal cases and for various SM backgrounds. Not surprisingly, backgrounds from SM final states involving  $b$  quarks produced in association with vector bosons to give sizeable  $\cancel{E}_T$  dominate: these include  $t\bar{t}$ ,  $Zb\bar{b}$ ,  $t\bar{t}Z$ , and  $Wb\bar{b}$  production. The signals peak at  $\sim 1400$ – $1600$  GeV depending on the wino mass, while the backgrounds are broader continua. We see that in favorable cases the signal, though not large, is comparable to the background in several bins, and it appears that this channel could make a contribution to the significance when the channels are combined.

### H. $\ell^\pm\ell^\pm + \cancel{E}_T$ channel

This channel is designed to catch very characteristic events with two same-sign dileptons coming from the leptonic decays of same-sign  $W$  bosons produced from the decays of pair-produced winos [67]. This signal—which is characteristic of light Higgsino models—has low rates but is interesting because it also has very low backgrounds from SM processes. In Ref. [59], it was shown that the discovery reach of the HL-LHC, via this single channel, extended to a wino mass of  $\sim 860$  GeV. Here, since we are exploring the wino reach that might be possible by combining several channels, we have reanalyzed the same-sign dilepton channel exploring harder cuts that might allow us to go out further in the wino mass

at the HL-LHC. Upon exploring various distributions, we require the additional cuts

- (1)  $|\eta(\ell)| < 2$ ,
- (2)  $\cancel{E}_T > 350$  GeV,
- (3)  $\Delta\phi(\ell\ell, \cancel{E}_T) > \pi/3$  where  $\Delta\phi$  is the transverse plane opening angle between the  $\vec{p}_T(\ell\ell)$  and  $\vec{\cancel{E}}_T$ , and
- (4)  $\Delta\phi(\ell_1, \cancel{E}_T) > \pi/4$  and  $\Delta\phi(\ell_2, \cancel{E}_T) > \pi/4$ .

The  $\cancel{E}_T$  cut allows us to probe the signal from TeV scale winos, and the angular cuts require that the  $\cancel{E}_T$  vector is well separated from the leptons.

In Fig. 10 we show the distribution of  $L_T \equiv |p_T(\ell_1)| + |p_T(\ell_2)| + |\cancel{E}_T|$  for the two signal cases and for dominant SM backgrounds after the analysis just described. We have checked that  $t\bar{t}$  production (not shown) makes a subdominant contribution to the signal. We see that though the signal rate is very small, the signal stands out above SM backgrounds for  $L_T > 800$ – $1000$  GeV. We emphasize that this channel is characteristic of models with light Higgsinos whose decay products are essentially invisible and would be absent in models where winos decayed to binos and Higgsino states are decoupled. We also stress that the signal has essentially no jet activity other than that from QCD radiation, and so should be readily distinguishable from the same-sign dilepton production via gluino [70–73] or squark [74] pair production.

## VI. REACH OF HL-LHC FOR EWINOS IN NATURAL SUSY

Now that we have settled on our strategy to probe winos via the eight channels discussed in Sec. V, it is possible to obtain the LHC discovery sensitivity should there be an excess of events above SM backgrounds, or the corresponding exclusion limit if no such excess is observed at the HL-LHC. We express this in terms of the largest value of  $m_{1/2}$  (or equivalently, the wino mass) that can be probed in the HL-LHC run which is envisaged to accumulate an integrated luminosity of  $3000 \text{ fb}^{-1}$ .

For each of the first seven channels we examine the binned  $m_{T2}$  or the transverse mass distributions shown in Figs. 3–9. For the same-sign dilepton +  $\cancel{E}_T$  channel, we examined the  $L_T$  distribution in Fig. 10. For exclusion of the wino signal, we assume that the true distribution we would observe in an experiment would correspond to a background only distribution. Upper limits on  $m_{1/2}$  are then evaluated using a modified frequentist  $CL_S$  method [75] with the profile likelihood ratio as the test statistic. The likelihood is built as a product of Poissonian terms for each of the bins in the distributions. A background systematic error is accounted for by introducing an independent nuisance parameter for each bin of each channel, and the likelihood is modified by log-normal terms to account for these nuisance parameters, with uncertainty that we take to be 25%. The largest value of  $m_{1/2}$  (or equivalently, the largest value of wino mass) that can be excluded at 95% CL is the

TABLE I. Statistical significance of the signal for each of the eight different signal channels for the model-line case with  $m_{1/2} = 1.3$  TeV at HL-LHC, assuming an integrated luminosity of  $3000 \text{ fb}^{-1}$ .

Signal channel	Significance (0% systematic)	Significance (25% systematic)
$Z(\rightarrow \ell^+\ell^-)B + E_T$	2.1	2.2
$h/Z(\rightarrow bb)B + E_T$	2.6	2.4
$BB + E_T$	1.60	0.4
$\ell h + E_T$	1.6	1.5
$\ell B_{W/Z} + E_T$	1.4	0.6
$Z(\ell^+\ell^-) + E_T$	1.2	1.2
$bb + E_T$	1.5	1.2
$\ell^\pm \ell^\pm + E_T$	2.4	2.4
combined	5.3	4.7

exclusion limit. For discovery, we assume that the distribution one would observe in an experiment corresponds to signal plus background. We then test this against the background only distribution for each value of  $m_{1/2}$ . If the background only hypothesis can be rejected at least the  $5\sigma$  level, we deem that the HL-LHC would discover winos with a mass corresponding to that choice of  $m_{1/2}$ . For both the exclusion and discovery limits, we use the asymptotic expansion for obtaining the median significance [76].<sup>12</sup>

To warm up, we begin by considering the relative importance of the eight channels introduced in Sec. V to the wino reach at the HL-LHC. The presence of a signal will distort the  $m_{T2}$ ,  $M_T$ , or  $L_T$  distributions illustrated in Sec. V. The magnitude of this distortion and its statistical significance depends on both the number of signal as well as the number of background events in optimally chosen bins, and the probability of the background fluctuating to the level of the signal can be translated into the number of “standard deviations.” Our results of this exercise are shown in Table I for the case with  $m_{1/2} = 1.3$  TeV along our model line, with statistical errors only as well as with an assumed 25% systematic error on the background: in this choice, we are guided by Fig. 9 of the ATLAS study Ref. [17]. We see that the  $h/Z(\rightarrow bb)B + E_T$  channel is the largest contributor, closely followed by the same-sign dilepton  $+E_T$  channel. The other channels individually make smaller contributions but combine to noticeably increase the significance. We see from Figs. 3 and 4 that the signal sticks out over the background (remember though that the background histograms are not stacked),

<sup>12</sup>We have checked that for every channel that we study there are at least ten (frequently significantly more) background events in the “sensitive regions” of the histograms in Figs. 3–10. This is large enough to justify the use of asymptotic formulas since for discovery (exclusion) we are concerned with fluctuations of the background (signal plus background).

but the higher signal rate leads to a somewhat better significance in the second case. When there is no systematic, we see that the  $BB + E_T$  channel remains competitive with the remaining channels in spite of the fact that the signal in Fig. 5 is buried under the background. As already noted, this is due to the large signal rate expected in this channel. Once systematic uncertainty is introduced, significance in channels that have a low  $S/B$  ratio such as  $BB + E_T$  and  $\ell B_{W/Z} + E_T$  channels is reduced significantly. Those with a high  $S/B$  ratio are more resilient even if large systematic is present. Although none of the channels individually provide even  $3\sigma$  evidence of a signal, we see from the table that by combining the eight channels one would attain a  $5\sigma$  significance if systematic uncertainties can be ignored.

The HL-LHC discovery reach and the 95% CL exclusion level after combining all the channels with statistical errors alone are shown in the upper panels of Figs. 11 and 12,

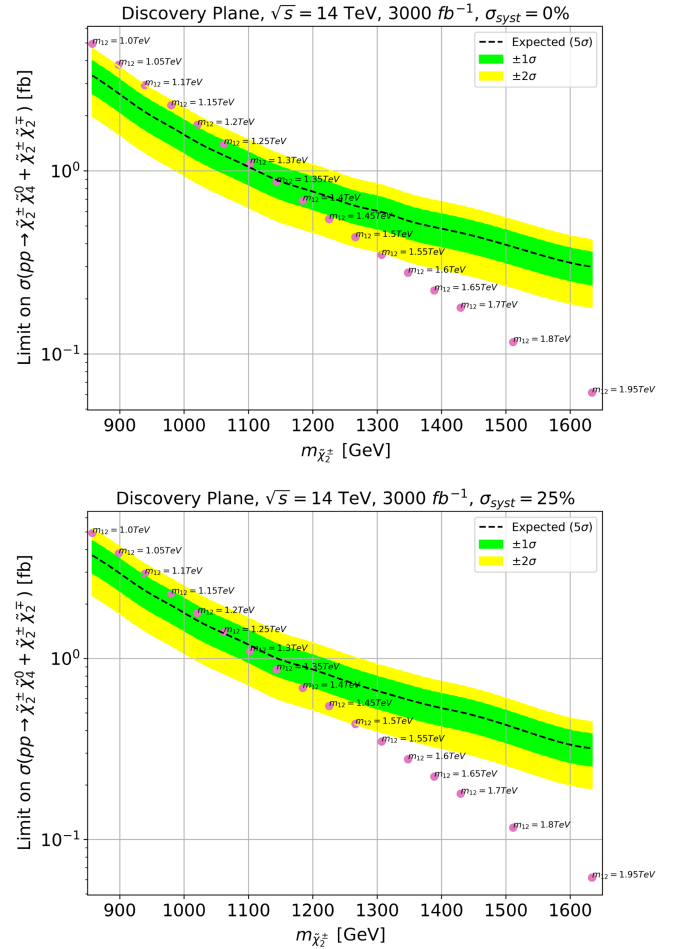


FIG. 11.  $5\sigma$  discovery reach of HL-LHC from wino pair production as a function of  $m_{1/2}$ , with other parameters as in Eq. (3), after combining the eight discovery channels detailed in the text. The upper panel shows the reach with statistical errors alone while the lower panel shows the reach assuming an additional 25% systematic error common to all the channels.

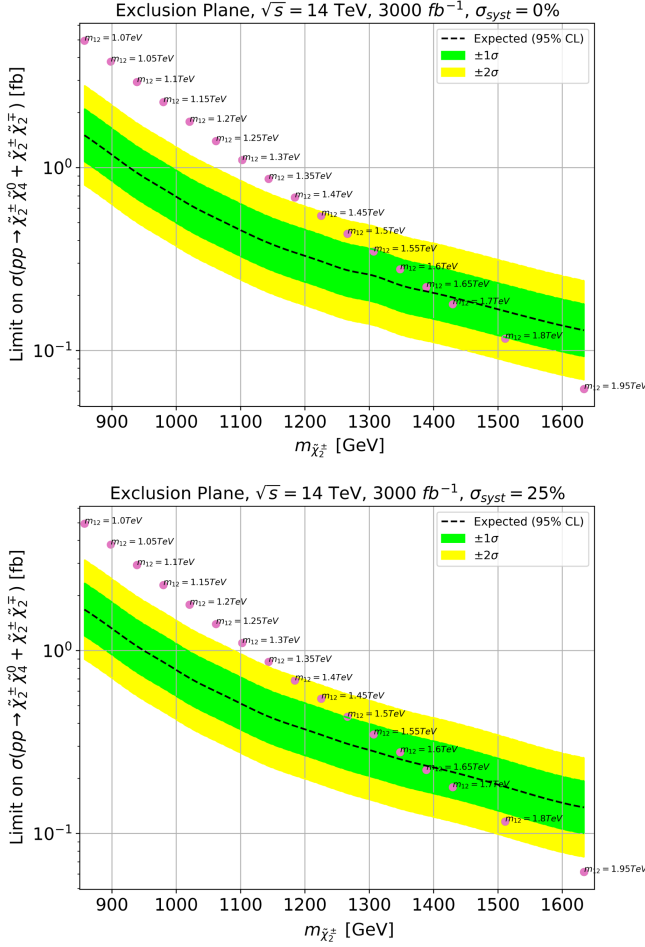


FIG. 12. The 95% CL exclusion limit of HL-LHC from wino pair production as a function of  $m_{1/2}$ , with other parameters as in Eq. (3), after combining the eight discovery channels detailed in the text. The upper panel shows the reach with statistical errors alone while the lower panel shows the reach assuming an additional 25% systematic error common to all the channels.

respectively. The systematic error is almost certainly channel dependent and difficult to evaluate. To illustrate its impact, however, we show in the bottom panels how these might be altered if we assume a common systematic error of 25% for all the channels. The minimum cross section for discovery/exclusion is shown by the black dashed line; following ATLAS and CMS, we denote by the green (yellow) bands how much this discovery/exclusion line might move due to background fluctuations at the  $1\sigma$  ( $2\sigma$ ) level. From Fig. 11, we see from the upper panel that the HL-LHC discovery limit for winos extends to a wino mass of about 1.15 TeV. From the lower panel, we see that with the assumed 25% common systematic uncertainty, the discovery limit drops by  $\sim 50$  GeV. Turning to Fig. 12, we project that experiments at the HL-LHC would be sensitive to a charged wino mass of almost 1.4 TeV. Although not shown, we have checked that even with a

100% systematic uncertainty on the background, the exclusion contour extends to  $m_{\tilde{\chi}_2^\pm} = 1.3$  TeV.

Before closing this section, we point out that we have considered the signal only from wino pair production in this paper even though the cross section for charged-wino production in association with a bino, shown in Fig. 1(c), is comparable to the cross section for the associated production of charged and neutral winos. The reason for this is that—for the channels with hadronically decaying  $W/Z/h$  bosons—our analysis cuts work best for boosted bosons. For the NUHM2 model with unified gaugino masses, the bino mass is about half the wino mass, and the boson daughters from bino decay have too small a boost to pass these cuts efficiently.

## VII. DO WINO SIGNALS LEAVE AN IMPRINT OF A LIGHT HIGGSINO?

Up to now, we have concentrated on the HL-LHC reach via signals from wino production in natural SUSY models. In this section, we ask whether it is possible to tell if the winos are indeed decaying to Higgsinos (as they must in natural SUSY models because  $|\mu|$  cannot be much larger than the weak scale) should signals for winos appear at the HL-LHC. We begin with a discussion of how the wino decay patterns would be altered from those discussed in Sec. IV if Higgsinos are very heavy and inaccessible via decays of winos; i.e., in models where the LSP is dominantly binolike. For simplicity of discussion, we assume  $|\mu| \gg M_2 \simeq 2M_1$ , and continue to take sfermions to be in the multi-TeV mass range. We also take  $m_A = 2$  TeV so that the additional Higgs bosons of the MSSM are also inaccessible via decays of the winos. This leads to an electroweak-ino spectrum that was in vogue in many early SUSY analyses performed within the so-called minimal supergravity framework (see, e.g., Ref. [77]) with  $\tilde{\chi}_1^0$  being binolike,  $\tilde{\chi}_1^\pm$  and  $\tilde{\chi}_2^0$  being winolike, and  $\tilde{\chi}_2^\pm$ ,  $\tilde{\chi}_3^0$ , and  $\tilde{\chi}_4^0$  being Higgsino-like, with a sizeable gap between  $m_{\tilde{\chi}_1^\pm} \simeq m_{\tilde{\chi}_2^0}$  and  $m_{\tilde{\chi}_1^0}$ .

In this case, the charged wino dominantly decays via  $\tilde{\chi}_1^\pm \rightarrow W\tilde{\chi}_1^0$ , this being the only two-body decay accessible to it. There are no two-body decays to a  $Z$  or to  $h$ . This is in sharp contrast to the situation shown in Fig. 2 where we saw that the wino state  $\tilde{\chi}_2^\pm$  decayed into  $W$ ,  $Z$  and  $h$  plus a quasi-invisible Higgsino with branching ratios of about 50%, 25%, and 25%, respectively.

Turning our attention to the neutral wino state  $\tilde{\chi}_2^0$ , we note that the decays  $\tilde{\chi}_2^0 \rightarrow h\tilde{\chi}_1^0$  and  $\tilde{\chi}_2^0 \rightarrow Z\tilde{\chi}_1^0$  are both kinematically accessible for TeV scale winos. Note, however, that the  $\tilde{\chi}_2^0 - h - \tilde{\chi}_1^0$  coupling can only occur due to the Higgsino component of  $\tilde{\chi}_1^0$  or  $\tilde{\chi}_2^0$ , and so is suppressed by a small mixing angle  $\sim m_Z/|\mu|$ . In contrast, since the  $Z$  couples to neutralinos only via the Higgsino components of

both the neutralinos (gauge invariance precludes a coupling of  $Z$  to neutral gauginos), the coupling to  $Z$  is suppressed by 2 factors of the small mixing angle. As a result, in models with  $|\mu| \gg M_2 \simeq 2M_1$ , the neutral wino decays almost exclusively via  $\tilde{\chi}_2^0 \rightarrow \tilde{\chi}_1^0 h$ ; i.e., the branching ratio for  $\tilde{\chi}_2^0 \rightarrow \tilde{\chi}_1^0 Z$  is *dynamically* suppressed.<sup>13</sup>

The upshot of this discussion is that in large  $|\mu|$  models (at least those with gaugino mass unification) *there cannot be a signal from wino production in those channels involving an identified high  $p_T$   $Z$  boson, whereas in models with light Higgsinos, these signals must be present.* Of the eight channels introduced in Sec. V, the channels 1, 2', and 6 clearly have an identified  $Z$  boson in them, where 2' here denotes channel 2 with  $80 \text{ GeV} < m_{bb} < 100 \text{ GeV}$ . Moreover,  $W^\pm W^\pm + \cancel{E}_T$  events required for events in channel 8 occur only if winos can decay into Higgsinos. A signal in channels 1, 2', 6, and 8 is thus a clear indication of light Higgsinos, assuming that the signal from the eight channels originates in the production of wino states at the HL-LHC.

To quantify this, we show in Fig. 13 the statistical significance of the signal above SM expectations as a function of the wino mass. The upper curve shows the result obtained by combining all eight channels, while the lower curve shows the result obtained including the channels with a clearly identified  $Z$  boson (channels 1, 2', 6, and 8). These are labeled as *light Higgsino specific channels* on the figure. A systematic uncertainty of 25% is included in this figure. We see that while the discovery reach of the HL-LHC with  $3000 \text{ fb}^{-1}$  extends to 1100 GeV, we interpret the lower curve as indicative of about  $3\sigma$  evidence for the existence of light Higgsinos out to a wino mass of 1200 GeV if we attribute the signal to arising from winos of supersymmetry.

We mention here that events with same sign dileptons could also arise from same-sign wino production via  $W^\pm W^\pm \rightarrow \tilde{\chi}_2^\pm \tilde{\chi}_2^\pm$  scattering: these events would be characterized by the presence of energetic jets in the high  $|\eta|$  region. Also, high  $p_T$   $Z$  bosons could arise in models with large  $|\mu|$  from heavy Higgsinos decaying to the lighter inos, or even from gluino and squark cascades as pointed out more than three decades ago [78]. Note that in either of

<sup>13</sup>We note that because of the gaugino mass unification assumption, the bino mass can never be neglected in the computation of the wino decay widths. As a result, neutral wino decays into the longitudinally polarized  $Z$  boson are not as enhanced as for the case of the Higgsino LSP discussed in Ref. [59] [see Eq. (B.61b) of Ref. [77]], and the branching ratio for  $\tilde{\chi}_2^0 \rightarrow \tilde{\chi}_1^0 Z$  decays remains small. We have checked that  $B(\tilde{\chi}_2^0 \rightarrow \tilde{\chi}_1^0 Z)$ , which also depends on mixing angles, is typically below  $\sim 5\%$  (10%) for a wino mass of 1.7 (3) TeV. This situation may be different in models without gaugino mass unification if the weak scale bino mass parameter is much smaller than the wino mass parameter.

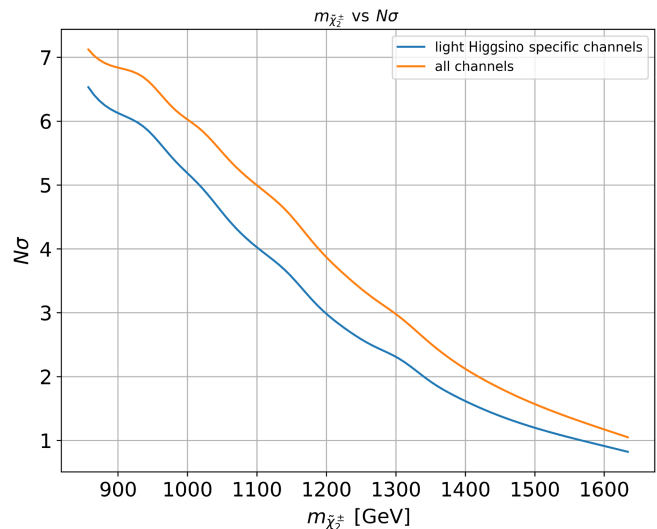


FIG. 13. The statistical significance for wino pair production as a function of  $m_{\tilde{\chi}_2^\pm}$ , with other parameters as in Eq. (3), after combining the eight discovery channels detailed in the text (upper curve), and combining only the light Higgsino specific channels with an identified  $Z$  boson (lower curve) including an additional 25% systematic error common to all the channels.

these cases, Higgsino states are necessary to get a  $Z$  boson daughter in the signal.<sup>14</sup> It is clear, however, that the event rates from heavy Higgsino cascades to winos would be much smaller than the corresponding rates expected from wino production in natural SUSY models. Gluino and squark events would be distinguished by very different event topologies from wino events studied in this paper. Events with high  $p_T$   $Z$  bosons, together with  $\ell^\pm \ell^\pm + \cancel{E}_T$  events with limited jet activity, will provide indirect evidence for the existence of light Higgsinos, should a wino signal be found at the LHC.

Instead of comparing with the SM as we do in Fig. 13, we considered a comparison of the natural SUSY model with an NUHM2 model with large  $\mu$  so that the bino is the LSP. In this case, the gaugino mass unification assumption reduces the wino-LSP mass gap from that in the natural SUSY model with  $\mu = 250 \text{ GeV}$ . Setting the bino-LSP mass to be 250 GeV, however, takes us close to the region currently excluded by the LHC for winos up to about 1 TeV. A comparison with the SM, keeping only the light Higgsino specific channels, seems to be the cleanest way to test for light Higgsinos.

<sup>14</sup>In principle, high  $p_T$   $Z$  bosons can also occur via decays of heavy sfermions if there is large intrageneration mixing [77], or if the super-GIM mechanism is not operative. Decays of heavy Higgs bosons, e.g.,  $A \rightarrow hZ$  could also lead to high  $p_T$   $Z$  bosons in an event. Both sfermion events as well as heavy Higgs boson events involving  $Z$  would be readily distinguishable from wino events.

Another point of concern may be that this evidence dwindles for wino masses not much above the current bounds from the LHC. While this is true for the HL-LHC, we believe that an examination of these light Higgsino specific channels is nonetheless important because the soft dilepton plus monojet signature which can produce direct evidence for light Higgsinos at the HL-LHC is very sensitive to the mass gap between  $\tilde{\chi}_1^0$  and  $\tilde{\chi}_2^0$ . In contrast, the signal with high  $p_T$   $Z$  bosons is insensitive to the size of the mass gap, and could prove important at a future hadron collider with larger energy and/or luminosity than the HL-LHC. At the very least, it provides complimentary, albeit indirect, evidence for the existence of light Higgsinos. It goes almost without saying that electron-positron colliders with sufficient center-of-mass energy would provide the most unambiguous evidence for light Higgsinos [79–83].

### VIII. SUMMARY AND CONCLUDING REMARKS

In this paper we have continued our exploration of the reach of the HL-LHC for superpartners in natural SUSY models, characterized by a value of the electroweak fine-tuning measure  $\Delta_{\text{EW}} < 30$ . In these scenarios, Higgsinos are expected to be below  $\sim 350$  GeV while other superpartners, including top squarks, could well be in the multi-TeV range, well beyond the reach of the LHC. While experiments at the HL-LHC may indeed be able to directly probe Higgsino signals via the monojet plus soft dilepton channel, the prospects for discovery are sensitive to the Higgsino mass gap and their discovery is not guaranteed for the entire range of SUSY parameters [84]. Indeed, discovery of natural SUSY is guaranteed only at future colliders, e.g., an electron-positron collider with a center-of-mass energy high enough to produce Higgsinos, or a high energy  $pp$  collider with an energy in excess of 27 TeV assuming it can accumulate an integrated luminosity of  $15 \text{ ab}^{-1}$  [51]. While it is not known whether either an  $e^+e^-$  or a hadron collider with the required energy will ever be constructed, there are clear plans to increase the luminosity of the LHC by an order of magnitude, and operate this machine to accumulate  $3000 \text{ fb}^{-1}$  of integrated luminosity over a decade. In this paper, we examine the discovery potential for winos of supersymmetry at the HL-LHC within the natural SUSY framework.

For winos in the 1–2 TeV range, the cross sections for wino pair production range between  $\mathcal{O}(1) \text{ fb}$  to  $\mathcal{O}(0.01) \text{ fb}$ , as discussed in Sec. III. For heavy sfermions, these cross sections are determined by the  $SU(2) \times U(1)$  gauge interactions and so are essentially fixed by the wino mass, independent of the SUSY model. However, wino decay patterns—and hence the signatures—depend on the nature of the LSP, and so are very different in natural SUSY from the more well-studied case of a bino LSP. Assuming

that matter sfermions and the additional Higgs bosons are significantly heavier than the wino, in natural SUSY heavy charged and neutral winos decay to on shell  $W$ ,  $Z$  and  $h$  bosons and an associated Higgsino with branching fractions in the ratio  $\sim 2:1:1$ ; see Fig. 2. In contrast, in models with a binolike LSP, the charged wino essentially always decays to a  $W$  boson and an LSP, while the neutral wino decays to an  $h$  boson and an LSP. Since the Higgsino mass gap is typically 4–15 GeV in natural SUSY models, the visible decay products of the daughter Higgsinos are too soft to be detected (without special effort) at hadron colliders, and wino pair production is signaled by  $VV$ ,  $Vh$ , and  $hh$  plus  $\cancel{E}_T$  events in natural SUSY models.

To facilitate our study of winos in natural SUSY models, we have identified eight experimentally distinct channels via which it would be possible to search for wino pair production in Sec. V. These channels depend on how the high  $p_T$   $W$ ,  $Z$  and  $h$  boson daughters of the TeV scale winos decay. For each of these channels, we identify cuts that enhance the signal relative to SM backgrounds from  $t\bar{t}$ ,  $t\bar{t}V$ ,  $t\bar{t}h$ ,  $VV$ ,  $hh$ ,  $VVV$ ,  $hhV$ ,  $V + \text{jets}$ , and  $Vh$  parton level processes. For each channel, we then plot one of the  $m_T$ ,  $m_{T2}$ , or  $L_T$  distributions for various signal cases and for SM backgrounds: these are shown in Figs. 3–10.

In Sec. VI we use these distributions to map out the  $5\sigma$  discovery and the 95% CL exclusion region for winos at the HL-LHC obtained after combining the signal from all eight channels. Table I shows the relative importance of each of these channels. Our final results for the HL-LHC reach and exclusion are summarized in Figs. 11 and 12, respectively. The upper panel shows the results with statistical errors alone, while the lower panel shows how these are affected if we assume a common systematic error of 25% for each of the eight channels. While experiments at the HL-LHC may be able to discover (exclude at 95% CL) wino masses up to 1.1 TeV (1.4 TeV), this is unfortunately a small part of the range allowed by natural SUSY. This should not be surprising because wino masses are relatively weakly constrained by naturalness considerations alone, and their discovery at the energy of the LHC would have to be somewhat fortuitous. While the HL-LHC can probe only a small part of the natural SUSY parameter space via wino searches, our discussion in Sec. VII shows that if a natural SUSY wino signal is seen at the LHC, it could potentially also provide indications for the existence of light Higgsinos: see Fig. 13. The point is that there are several Higgsino-specific channels (labeled 1, 2', 6, and 8 in the text) where instead there would be only a tiny signal from wino production in any model with a bino LSP. While the range of parameters where this may be possible at the HL-LHC is small, we find it very interesting that the presence of light Higgsinos may reveal itself at a hadron collider via signals from wino pair production alone. This could be critical if the

next accelerator facility is a higher energy/luminosity hadron collider and the Higgsino mass gap is too small for the monojet plus soft dilepton signal from Higgsino pair production to be observable. At the very least, the signal from winos yields an indirect confirmation of the existence of light Higgsinos.

## ACKNOWLEDGMENTS

This material is based upon work supported by the U.S. Department of Energy, Office of Science, Office of High Energy Physics under Award No. DE-SC-0009956. V. B. gratefully acknowledges support from the William F. Vilas estate.

- 
- [1] E. Witten, Dynamical breaking of supersymmetry, *Nucl. Phys.* **B188**, 513 (1981).
- [2] S. Dimopoulos and H. Georgi, Softly broken supersymmetry and SU(5), *Nucl. Phys.* **B193**, 150 (1981).
- [3] N. Sakai, Naturalness in supersymmetric guts, *Z. Phys. C* **11**, 153 (1981).
- [4] R. K. Kaul and P. Majumdar, Cancellation of quadratically divergent mass corrections in globally supersymmetric spontaneously broken gauge theories, *Nucl. Phys.* **B199**, 36 (1982).
- [5] G. Aad *et al.*, Observation of a new particle in the search for the Standard Model Higgs boson with the ATLAS detector at the LHC, *Phys. Lett. B* **716**, 1 (2012).
- [6] S. Chatrchyan *et al.*, Observation of a new boson at a mass of 125 GeV with the CMS experiment at the LHC, *Phys. Lett. B* **716**, 30 (2012).
- [7] F. Vissani, Do experiments suggest a hierarchy problem?, *Phys. Rev. D* **57**, 7027 (1998).
- [8] G. Aad *et al.*, Search for squarks and gluinos in final states with one isolated lepton, jets, and missing transverse momentum at  $\sqrt{s} = 13$  with the ATLAS detector, *Eur. Phys. J. C* **81**, 600 (2021).
- [9] G. Aad *et al.*, Search for supersymmetry in final states with missing transverse momentum and three or more b-jets in 139 fb<sup>-1</sup> of proton-proton collisions at  $\sqrt{s} = 13$  TeV with the ATLAS detector, *Eur. Phys. J. C* **83**, 561 (2023).
- [10] A. M. Sirunyan *et al.*, Searches for physics beyond the standard model with the  $M_{T2}$  variable in hadronic final states with and without disappearing tracks in proton-proton collisions at  $\sqrt{s} = 13$  TeV, *Eur. Phys. J. C* **80**, 3 (2020).
- [11] A. M. Sirunyan *et al.*, Search for top squark production in fully-hadronic final states in proton-proton collisions at  $\sqrt{s} = 13$  TeV, *Phys. Rev. D* **104**, 052001 (2021).
- [12] A. Tumasyan *et al.*, Search for electroweak production of charginos and neutralinos at  $s = 13$  TeV in final states containing hadronic decays of WW, WZ, or WH and missing transverse momentum, *Phys. Lett. B* **842**, 137460 (2023).
- [13] A. Tumasyan *et al.*, Search for chargino-neutralino production in events with Higgs and W bosons using 137 fb<sup>-1</sup> of proton-proton collisions at  $\sqrt{s} = 13$  TeV, *J. High Energy Phys.* **10** (2021) 045.
- [14] A. Tumasyan *et al.*, Search for electroweak production of charginos and neutralinos in proton-proton collisions at  $\sqrt{s} = 13$  TeV, *J. High Energy Phys.* **04** (2022) 147.
- [15] S. Chatrchyan *et al.* (CMS Collaboration) Combined search for electroweak production of winos, binos, higgsinos, and sleptons in proton-proton collisions at  $\sqrt{s} = 13$  TeV, Report No. CMS-PAS-SUS-21-008, 2023.
- [16] G. Aad *et al.*, Search for direct production of electroweakinos in final states with one lepton, missing transverse momentum and a Higgs boson decaying into two  $b$ -jets in  $pp$  collisions at  $\sqrt{s} = 13$  TeV with the ATLAS detector, *Eur. Phys. J. C* **80**, 691 (2020).
- [17] G. Aad *et al.*, Search for charginos and neutralinos in final states with two boosted hadronically decaying bosons and missing transverse momentum in  $pp$  collisions at  $\sqrt{s} = 13$  TeV with the ATLAS detector, *Phys. Rev. D* **104**, 112010 (2021).
- [18] G. Aad *et al.*, Search for direct pair production of sleptons and charginos decaying to two leptons and neutralinos with mass splittings near the W-boson mass in  $\sqrt{s} = 13$  TeV  $pp$  collisions with the ATLAS detector, *J. High Energy Phys.* **06** (2023) 031.
- [19] G. Aad *et al.*, Searches for new phenomena in events with two leptons, jets, and missing transverse momentum in 139 fb<sup>-1</sup> of  $\sqrt{s} = 13$  TeV  $pp$  collisions with the ATLAS detector, *Eur. Phys. J. C* **83**, 515 (2023).
- [20] J. R. Ellis, K. Enqvist, D. V. Nanopoulos, and F. Zwirner, Observables in low-energy superstring models, *Mod. Phys. Lett. A* **01**, 57 (1986).
- [21] R. Barbieri and G. F. Giudice, Upper bounds on supersymmetric particle masses, *Nucl. Phys.* **B306**, 63 (1988).
- [22] S. Dimopoulos and G. F. Giudice, Naturalness constraints in supersymmetric theories with nonuniversal soft terms, *Phys. Lett. B* **357**, 573 (1995).
- [23] J. L. Feng, Naturalness and the status of supersymmetry, *Annu. Rev. Nucl. Part. Sci.* **63**, 351 (2013).
- [24] H. Baer, V. Barger, D. Martinez, and S. Salam, Practical naturalness and its implications for weak scale supersymmetry, *Phys. Rev. D* **108**, 035050 (2023).
- [25] H. Baer, V. Barger, and D. Mickelson, How conventional measures overestimate electroweak fine-tuning in supersymmetric theory, *Phys. Rev. D* **88**, 095013 (2013).
- [26] A. Mustafayev and X. Tata, Supersymmetry, naturalness, and light Higgsinos, *Indian J. Phys.* **88**, 991 (2014).
- [27] H. Baer, V. Barger, P. Huang, D. Mickelson, A. Mustafayev, and X. Tata, Radiative natural supersymmetry: Reconciling electroweak fine-tuning and the Higgs boson mass, *Phys. Rev. D* **87**, 115028 (2013).

- [28] H. Baer, V. Barger, and D. Martinez, Comparison of SUSY spectra generators for natural SUSY and string landscape predictions, *Eur. Phys. J. C* **82**, 172 (2022).
- [29] A. Dedes and P. Slavich, Two loop corrections to radiative electroweak symmetry breaking in the MSSM, *Nucl. Phys.* **B657**, 333 (2003).
- [30] K. J. Bae, H. Baer, V. Barger, and D. Sengupta, Revisiting the SUSY  $\mu$  problem and its solutions in the LHC era, *Phys. Rev. D* **99**, 115027 (2019).
- [31] H. Baer, V. Barger, P. Huang, A. Mustafayev, and X. Tata, Radiatively natural SUSY with a 125 GeV Higgs boson, *Phys. Rev. Lett.* **109**, 161802 (2012).
- [32] H. Baer, V. Barger, and S. Salam, Naturalness versus stringy naturalness (with implications for collider and dark matter searches), *Phys. Rev. Res.* **1**, 023001 (2019).
- [33] V. Agrawal, S. M. Barr, J. F. Donoghue, and D. Seckel, Anthropic considerations in multiple domain theories and the scale of electroweak symmetry breaking, *Phys. Rev. Lett.* **80**, 1822 (1998).
- [34] H. Baer, V. Barger, S. Salam, D. Sengupta, and K. Sinha, Status of weak scale supersymmetry after LHC Run 2 and ton-scale noble liquid WIMP searches, *Eur. Phys. J. Spec. Top.* **229**, 3085 (2020).
- [35] H. Baer, V. Barger, and M. Savoy, Upper bounds on sparticle masses from naturalness or how to disprove weak scale supersymmetry, *Phys. Rev. D* **93**, 035016 (2016).
- [36] H. Baer, V. Barger, J. S. Gainer, P. Huang, M. Savoy, D. Sengupta, and X. Tata, Gluino reach and mass extraction at the LHC in radiatively-driven natural SUSY, *Eur. Phys. J. C* **77**, 499 (2017).
- [37] X. Cid Vidal *et al.*, Report from working group 3: Beyond the Standard Model physics at the HL-LHC and HE-LHC, *CERN Yellow Rep. Monogr.* **7**, 585 (2019).
- [38] H. Baer, V. Barger, J. Dutta, D. Sengupta, and K. Zhang, Top squarks from the landscape at high luminosity LHC, *Phys. Rev. D* **108**, 075027 (2023).
- [39] H. Baer, V. Barger, and P. Huang, Hidden SUSY at the LHC: The light Higgsino-world scenario and the role of a lepton collider, *J. High Energy Phys.* **11** (2011) 031.
- [40] Z. Han, G. D. Kribs, A. Martin, and A. Menon, Hunting quasidegenerate Higgsinos, *Phys. Rev. D* **89**, 075007 (2014).
- [41] H. Baer, A. Mustafayev, and X. Tata, Monojet plus soft dilepton signal from light Higgsino pair production at LHC14, *Phys. Rev. D* **90**, 115007 (2014).
- [42] C. Han, D. Kim, S. Munir, and M. Park, Accessing the core of naturalness, nearly degenerate Higgsinos, at the LHC, *J. High Energy Phys.* **04** (2015) 132.
- [43] G. Aad *et al.*, Searches for electroweak production of supersymmetric particles with compressed mass spectra in  $\sqrt{s} = 13$  TeV  $pp$  collisions with the ATLAS detector, *Phys. Rev. D* **101**, 052005 (2020).
- [44] A. Tumasyan *et al.*, Search for supersymmetry in final states with two or three soft leptons and missing transverse momentum in proton-proton collisions at  $\sqrt{s} = 13$  TeV, *J. High Energy Phys.* **04** (2022) 091.
- [45] H. Baer, V. Barger, M. Padeffke-Kirkland, and X. Tata, Naturalness implies intra-generational degeneracy for decoupled squarks and sleptons, *Phys. Rev. D* **89**, 037701 (2014).
- [46] H. Baer, V. Barger, and D. Sengupta, Landscape solution to the SUSY flavor and  $CP$  problems, *Phys. Rev. Res.* **1**, 033179 (2019).
- [47] H. Baer, V. Barger, A. Lessa, W. Sreethawong, and X. Tata, Wh plus missing- $E_T$  signature from gaugino pair production at the LHC, *Phys. Rev. D* **85**, 055022 (2012).
- [48] G. Aad *et al.*, Search for chargino-neutralino pair production in final states with three leptons and missing transverse momentum in  $\sqrt{s} = 13$  TeV  $pp$  collisions with the ATLAS detector, *Eur. Phys. J. C* **81**, 1118 (2021).
- [49] M. Aaboud *et al.*, Search for chargino and neutralino production in final states with a Higgs boson and missing transverse momentum at  $\sqrt{s} = 13$  TeV with the ATLAS detector, *Phys. Rev. D* **100**, 012006 (2019).
- [50] L. M. Carpenter, H. Gilmer, J. Kawamura, and T. Murphy, Taking aim at the wino-higgsino plane with the LHC, [arXiv:2309.07213](https://arxiv.org/abs/2309.07213).
- [51] H. Baer, V. Barger, J. S. Gainer, D. Sengupta, H. Serce, and X. Tata, LHC luminosity and energy upgrades confront natural supersymmetry models, *Phys. Rev. D* **98**, 075010 (2018).
- [52] H. Baer, V. Barger, P. Huang, D. Mickelson, A. Mustafayev, W. Sreethawong, and X. Tata, Radiatively driven natural supersymmetry at the LHC, *J. High Energy Phys.* **12** (2013) 013; **06** (2015) 053.
- [53] D. Matalliotakis and H. P. Nilles, Implications of nonuniversality of soft terms in supersymmetric grand unified theories, *Nucl. Phys.* **B435**, 115 (1995).
- [54] J. R. Ellis, K. A. Olive, and Y. Santoso, The MSSM parameter space with nonuniversal Higgs masses, *Phys. Lett. B* **539**, 107 (2002).
- [55] P. Nath and R. L. Arnowitt, Nonuniversal soft SUSY breaking and dark matter, *Phys. Rev. D* **56**, 2820 (1997).
- [56] F. E. Paige, S. D. Protopopescu, H. Baer, and X. Tata, ISAJET 7.69: A Monte Carlo event generator for  $pp$ , anti- $p$ ,  $p$ , and  $e + e -$  reactions, [arXiv:hep-ph/0312045](https://arxiv.org/abs/hep-ph/0312045).
- [57] H. Baer, V. Barger, X. Tata, and K. Zhang, Prospects for heavy neutral SUSY Higgs scalars in the hMSSM and natural SUSY at LHC upgrades, *Symmetry* **14**, 2061 (2022).
- [58] W. Beenakker, R. Hopker, and M. Spira, PROSPINO: A program for the production of supersymmetric particles in next-to-leading order QCD, [arXiv:hep-ph/9611232](https://arxiv.org/abs/hep-ph/9611232).
- [59] H. Baer, V. Barger, J. S. Gainer, M. Savoy, D. Sengupta, and X. Tata, Aspects of the same-sign diboson signature from wino pair production with light Higgsinos at the high luminosity LHC, *Phys. Rev. D* **97**, 035012 (2018).
- [60] P. Z. Skands *et al.*, SUSY Les Houches accord: Interfacing SUSY spectrum calculators, decay packages, and event generators, *J. High Energy Phys.* **07** (2004) 036.
- [61] T. Sjostrand, S. Mrenna, and P. Z. Skands, PYTHIA 6.4 physics and manual, *J. High Energy Phys.* **05** (2006) 026.
- [62] J. Alwall, M. Herquet, F. Maltoni, O. Mattelaer, and T. Stelzer, MadGraph 5: Going beyond, *J. High Energy Phys.* **06** (2011) 128.
- [63] D. de Florian *et al.*, *Handbook of LHC Higgs Cross Sections: 4. Deciphering the Nature of the Higgs Sector* (CERN, Geneva, 2016), Vol. 2.
- [64] J. M. Campbell, R. K. Ellis, and C. Williams, Vector boson pair production at the LHC, *J. High Energy Phys.* **07** (2011) 018.

- [65] J. de Favereau, C. Delaere, P. Demin, A. Giammanco, V. Lemaître, A. Mertens, and M. Selvaggi, DELPHES 3, A modular framework for fast simulation of a generic collider experiment, *J. High Energy Phys.* **02** (2014) 057.
- [66] D. Krohn, J. Thaler, and L.-T. Wang, Jet trimming, *J. High Energy Phys.* **02** (2010) 084.
- [67] H. Baer, V. Barger, P. Huang, D. Mickelson, A. Mustafayev, W. Sreethawong, and X. Tata, Same sign diboson signature from supersymmetry models with light Higgsinos at the LHC, *Phys. Rev. Lett.* **110**, 151801 (2013).
- [68] A. Barr, C. Lester, and P. Stephens,  $m_{T2}$ : The truth behind the glamour, *J. Phys. G* **29**, 2343 (2003).
- [69] V.D. Barger, A. D. Martin, and R. J. N. Phillips, Evidence for the t quark in anti-p p collider data, *Phys. Lett. B* **125**, 339 (1983).
- [70] R. M. Barnett, J. F. Gunion, and H. E. Haber, Gluino decay patterns and signatures, *Phys. Rev. D* **37**, 1892 (1988).
- [71] H. Baer, X. Tata, and J. Woodside, Gluino cascade decay signatures at the tevatron collider, *Phys. Rev. D* **41**, 906 (1990).
- [72] H. Baer, X. Tata, and J. Woodside, Multi-lepton signals from supersymmetry at hadron super colliders, *Phys. Rev. D* **45**, 142 (1992).
- [73] R. M. Barnett, J. F. Gunion, and H. E. Haber, Discovering supersymmetry with like sign dileptons, *Phys. Lett. B* **315**, 349 (1993).
- [74] H. Baer, C.-h. Chen, F. Paige, and X. Tata, Signals for minimal supergravity at the CERN Large Hadron Collider. 2: Multi-lepton channels, *Phys. Rev. D* **53**, 6241 (1996).
- [75] A. L. Read, Presentation of search results: The  $CL_s$  technique, *J. Phys. G* **28**, 2693 (2002).
- [76] G. Cowan, K. Cranmer, E. Gross, and O. Vitells, Asymptotic formulae for likelihood-based tests of new physics, *Eur. Phys. J. C* **71**, 1554 (2011).
- [77] H. Baer and X. Tata, *Weak Scale Supersymmetry: From Superfields to Scattering Events* (Cambridge University Press, Cambridge, England, 2006).
- [78] H. Baer, X. Tata, and J. Woodside,  $Z^0 + \text{jets} + p_T$  events as a signal for supersymmetry at the Fermilab Tevatron collider, *Phys. Rev. D* **42**, 1450 (1990).
- [79] H. Baer, V. Barger, D. Mickelson, A. Mustafayev, and X. Tata, Physics at a Higgsino factory, *J. High Energy Phys.* **06** (2014) 172.
- [80] A. Arbey *et al.*, Physics at the  $e^+e^-$  linear collider, *Eur. Phys. J. C* **75**, 371 (2015).
- [81] H. Baer, M. Berggren, K. Fujii, S.-L. Lehtinen, J. List, T. Tanabe, and J. Yan, Naturalness and light Higgsinos: A powerful reason to build the ILC, *Proc. Sci. ICHEP2016* (2016) 156 [arXiv:1611.02846].
- [82] S.-L. Lehtinen, H. Baer, M. Berggren, J. List, K. Fujii, J. Yan, and T. Tanabe, Naturalness and light Higgsinos: Why ILC is the right machine for SUSY discovery, *Proc. Sci. EPS-HEP2017* (2017) 306 [arXiv:1710.02406].
- [83] H. Baer, M. Berggren, K. Fujii, J. List, S.-L. Lehtinen, T. Tanabe, and J. Yan, ILC as a natural SUSY discovery machine and precision microscope: From light Higgsinos to tests of unification, *Phys. Rev. D* **101**, 095026 (2020).
- [84] H. Baer, V. Barger, S. Salam, D. Sengupta, and X. Tata, The LHC Higgsino discovery plane for present and future SUSY searches, *Phys. Lett. B* **810**, 135777 (2020).